liquids

MDPI

Review

How the Concept of Solvent Polarity Investigated with Solvatochromic Probes Helps Studying Intermolecular Interactions

Heinz Langhals

Department of Chemistry, LMU University of Munich, Butenandtstr. 13, 81377 Munich, Germany; langhals@lrz.uni-muenchen.de

Abstract: Intermolecular interactions form the basis of the properties of solvents, such as their polarity, and are of central importance for chemistry; such interactions are widely discussed. Solvent effects were reported on the basis of various polarity probes with the $E_T(30)$ polarity scale of Dimroth and Reichardt being of special interest because of its sensitivity, precise measurability and other advantages, and has been used for the investigation of solvent interactions. A two-parameter equation for the concentration dependence of medium effects has been developed, providing insights into structural changes in liquid phases. Moving from condensed gases to binary solvent mixtures, where the property of one solvent can be continuously transformed to the other, it was shown how the polarity of a solvent can be composed from the effect of polar functional groups and other structural elements that form the matrix. Thermochromism was discussed as well as the effect of very long-range interactions. Practical applications were demonstrated.

Keywords: solvent polarity scales; $E_T(30)$ scale; condensed phases; binary mixtures; solvent structure

Citation: Langhals, H. How the Concept of Solvent Polarity Investigated with Solvatochromic Probes Helps Studying Intermolecular Interactions. *Liquids* **2023**, *3*, 481–511. https://doi.org/10.3390/liquids3040031

Academic Editors: William E. Acree, Jr., Franco Cataldo and Enrico Bodo

Received: 18 October 2023
Revised: 28 November 2023
Accepted: 1 December 2023
Published: 6 December 2023

1. Introduction

Most chemical syntheses were carried out in the liquid phases [1] where the average distances between molecules are small [2]. Noncovalent intermolecular interactions [3] are important in such condensed phases; they dominate the properties of chemical materials, and will subsequently be analyzed below. Adjusting the pressure of gases is a useful method for setting intermolecular distances and allows the systematic study of such effects.

2. General Intermolecular Interactions

The impact of a molecular chemical material such as the pressure p of gases depends on the numbers of particles in a volume, more conveniently indicated by the molar concentration c. Starting from highly diluted gases with essentially independent particles, the impact p is expected to be proportional to the concentration c giving the differential Equation (1).

$$dp = const_1 \cdot dc \quad (1)$$

As the concentration increases, the impact is changed more and more due to interactions of the particles, and the changes are expected to increase with the concentration of particles. Inverse proportionality implies a basic approach leading to the differential Equation (2), where the constant E stands for the energetic effect of c on p.

$$dp = E/c \cdot dc \quad (2)$$

Multiplying Equation (2) by c and dividing by the scaling factor c^* for the discrimination between the two extrema of Equations (1) and (2) and adjusting the dimensions yields Equation (3), where $c = 0$ can be included ($E/c^* = const_2$).

$$c/c^* \cdot dp = const_2 \cdot dc \tag{3}$$

The differential Equation (4) results from the addition of Equations (1) and (3) and the subsequent separation [4] of the variables p and c.

$$dp = \frac{const_2}{\left(\frac{c}{c*} + 1\right)} \, dc \tag{4}$$

Finally, Equation (5) is obtained by the integration of Equation (4) with the integration constant p_o; the latter is zero for diluted gases because the pressure p vanishes for infinite dilution of gases.

$$p = E \cdot \ln\left(\frac{c}{c*} + 1\right) + p_o \tag{5}$$

Equation (5) ends up in the ideal gas equation for diluted gases by a Taylor series expansion and truncation after the linear term forming Equation (6), where $c << c^*$ and the concentration c is the number of moles n over the volume V.

$$p \approx \frac{E}{(c + c*)} \cdot c \approx \frac{E}{c*} \cdot c = \frac{E \; n}{c* \; V} \tag{6}$$

Thus, the ideal gas equation (7) is obtained with $R \cdot T = E/c^*$.

$$p \cdot V \approx n \cdot \frac{E}{c*} = n \cdot R \cdot T \tag{7}$$

Equation (5) is an exact description [5] of the concentration dependence of the pressure of gases such as is shown for the precisely measured isotherms by Michels and Michels [6]. A typical linear correlation (performance of target to actual comparison) according to Equation (5) is shown in Figure 1 (a high accuracy of the linear correlation is achieved where deviations from experimental data are within 10 to about 20 ppm).

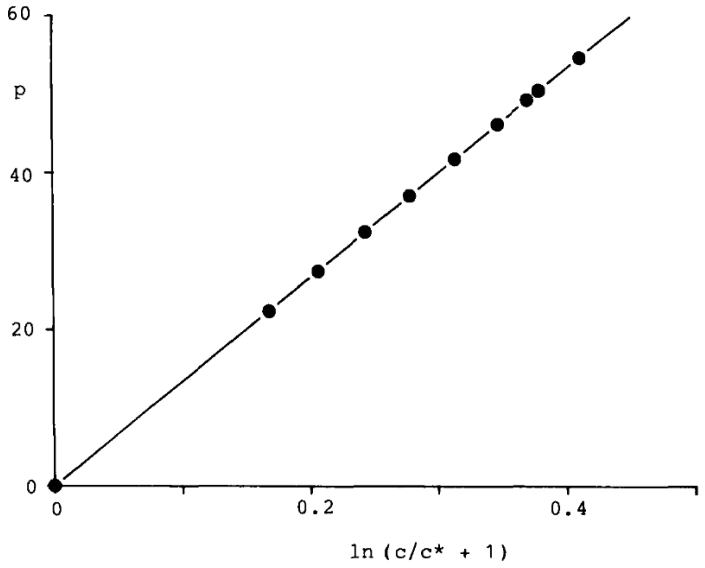

Figure 1. Typical linear correlation between p and ln (c/c^* + 1) according to Equation (5): CO_2 at 75.260 °C, c < 3.1 mol·L^{-1}; E = 133.4 at, c^* = 4.5 mol·L^{-1}, r = 0.999 998, n = 10; deviations in the correlation from experimental data of 10 until 20 ppm.

When the CO_2 concentration c exceeds a threshold value c_k(I-II) of 3.1 mol·L^{-1}, the dependence on the pressure in the low concentration region I changes abruptly to reach the concentration region II (see Figure 2). Equation (5) is also valid for region II, but with different parameters E and c^*, and p_o is different from 0.

$$p = p_o \cdot e^{E \cdot c} + p^* \tag{8}$$

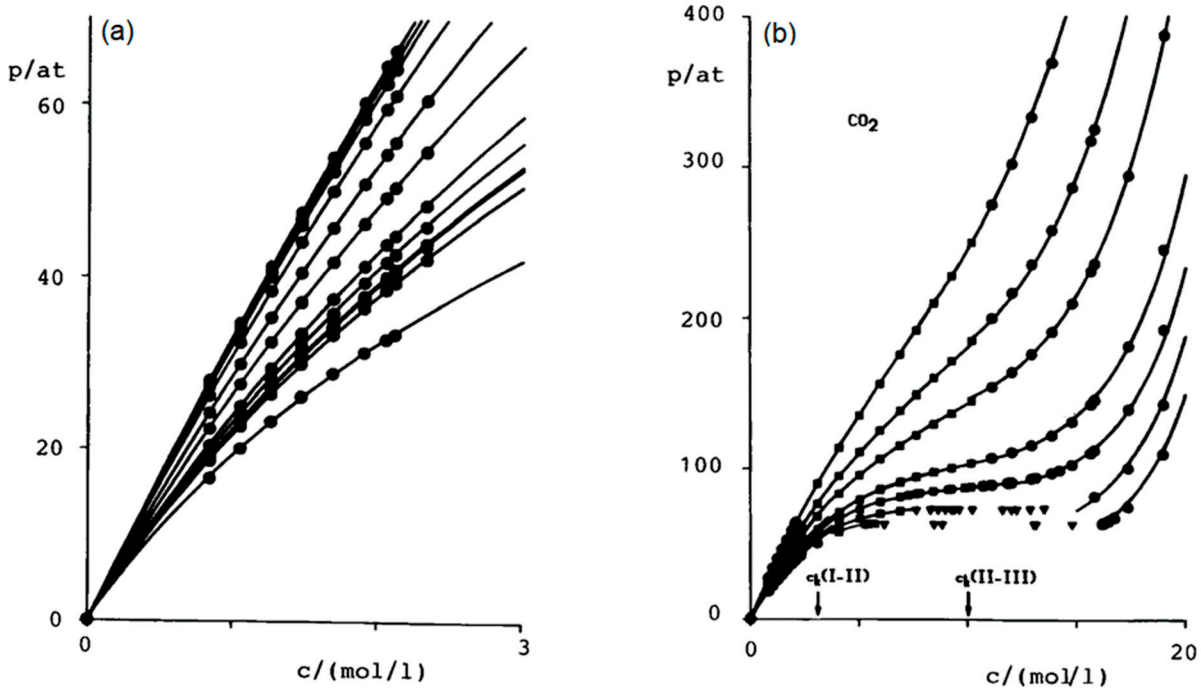

Figure 2. Diagram of state of CO_2: Discontinuous measurements were taken from Refs. [6–8], and curves were calculated [5] by means of Equations (5) and (8) and the application of the method of least squares to fit the experimental data. Measurements at very high pressure were included, but not shown in the right-hand diagram for graphical clarity. Temperatures (rounded): 25, 32, 40, 50, 75, 100, and 140 °C (see Ref. [9]) c_k(I-II) ≅ 3.1 mol·L^{-1} (concentration for the change from solvent structure I to II), c_k(II-III) ≅ 10 mol·L^{-1} (concentration for the change from solvent structure II to III). (**a**) Enlarged region I (c < 3.1 mol·L^{-1}). (**b**) Complete region I, II, and III; filled circles for region I and III, squares for region II, triangles for the biphasic region.

At even higher pressure, when c exceeds c_k(II-III) of 10 mol·L^{-1} the region III is reached. There, an exponential increase in p with concentration c was found and can be described by Equation (8) where p^* means a base pressure.

This more generally observed behavior of gases was interpreted in terms of structural changes in the medium; such effects are also considered to be fundamentally important for non-covalent interactions in solvent effects and will be more differentiated. The concentration c_k(I-II) for the transition from region I to region II of about 3.1 mol·L^{-1} corresponds to an edge length of 8.1 Å of a cube for one molecule, with mean intermolecular distance of 4.5 Å because of the statistical molecular movement [2]. This means about twice the molecular length between the nuclei of oxygen of 2.3 Å [10]. The concentration c_k(II-III) for the transition from region II to region III of about 10 mol·L^{-1} corresponds cube lengths of 5.5 Å and a mean intermolecular distance of 3.0 Å, not far away from the molecular dimensions and the intermolecular distance of 2.76 Å between the oxygen atoms in solid CO_2. There is a minimal restriction of the molecular motion in the region I, with a comparably abrupt change to permanent molecular contacts in region II. Finally, when c_k(II-III) is exceeded, the molecules are essentially densely packed, with further increases in concentration and density, respectively, is restricted by the prevailing effects of molecular compressibility,

causing an exponential increase in pressure. The formation of the liquid phase is observed in region II. This may be due to limited miscibility of densely packed molecular aggregates with loosely packed assemblies. The surface tension between such structures is responsible for the formation of two phases, becomes smaller with an increasing temperature, and with lowering the range of two phases, and finally vanishes at the critical point [11] at 31.0 °C for carbon dioxide.

Further information can be obtained from the temperature dependence of the parameters of Equation (5). The values of E and c^* in region I increase monotonically and smoothly with temperature T (see Figure 3), while in region II a slight increase is observed at lower temperatures, rising rapidly between 70 and 120 °C and increasing again slightly when this range is exceeded (this behavior is clearly observed, even being appreciable above the critical point of 31.0 °C). The influence of the temperature is interpreted in terms of region I essentially being dominated by isolated molecules, whereas region II has a complex dynamic arrangement of isolated molecules and aggregates. As a result, two phases formed at low temperatures due to their limited miscibility which at higher temperatures cause the rapid change in parameters shown in the inset of Figure 3, for which thermally induced dissociation of such aggregates is held responsible; the latter resembles the melting of clusters. Such assemblies are important for solvent effects and will be further discussed below.

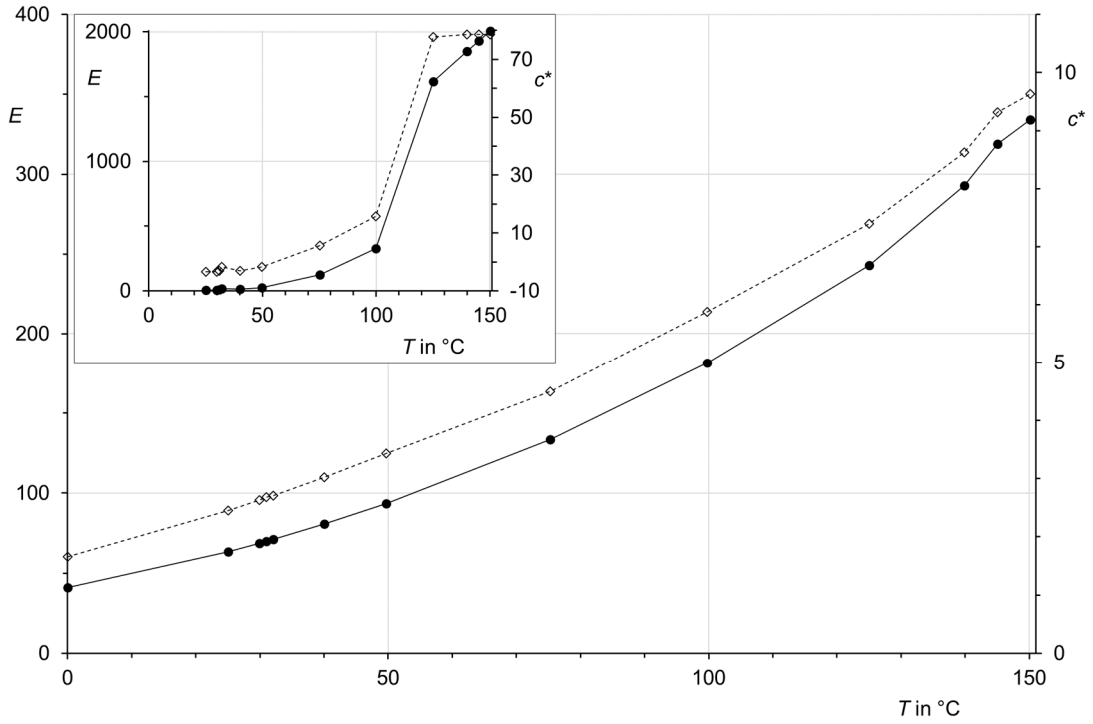

Figure 3. Temperature dependence (T) of the parameters E (solid curve and filled circles) and c^* (dashed curves and open diamonds) of Equation (5) for CO_2 and region I. Inset: parameters for region II.

3. General Solvent Effects

Condensed phases are widely used as media in chemistry and technology. Liquid phases are not only obviously used as solvents for an easier and more efficient handling of dissolved solids and to disperse them until the molecular level, but are also capable of interacting with substrates and imparting new properties through solvation. For example, the handling of the ethyl anion is very difficult in the gas phase because of the strongly exothermic tendency to lose one electron to form the ethyl radical [12,13]; on the other hand, a complexed and solvated ethyl anion such as the ethyl Grignard reagent [14] in

ether is fully stable and applied in routine preparative chemistry. Moreover, an appreciable influence of solvents on the rate of chemical reactions was found, documented early on by Berthelot [15] in esterification reactions. More extended investigations [16] were made by Menschutkin, who studied the quarternization [17,18] of triethylamine [19]; he not only found a considerable influence of the solvent on the reaction rate, but also noted strong effects due to the ions involved. The polarity of a medium seemed to be of central importance. Menschutkin's system was not ideal for the general study of solvent effects on chemical reaction rates because the effects involve both the electrophilic substrate for nucleophilic substitution reactions and the nucleophile itself; the separation of individual effects becomes difficult. Clausius Mossotti [20] and Kirkwood [21,22] took a physical approach to solvent effects using the relative dielectric permittivity (dielectric constant ε_r) as the fundamental physical property of a medium in which the solute occupies a spherical or more ellipsoidal volume in the homogenous solvent. The local electric field of the solute causes a polarization of the medium with pronounced effects of charged particles. Debye [23,24] described two extrema of polarization, the orientation polarization where the positions of atomic nuclei are altered, and the shift polarization when charge separation is induced by displacement of electrons only. Orientation polarization dominates in media consisting of sufficiently large dipoles and can be determined using the static permittivity or at low frequencies compared with the correlation time of molecular orientation; the Clausius–Mossotti function (Figure 4) was derived (solute occupies a spherical volume) to describe the effect proportional to $(\varepsilon_r - 1)/(\varepsilon_r + 2)$. Higher frequencies as in the optical range are useful for determining shift polarization because the comparably heavy atomic nuclei can no more follow an external field; the index of refraction is a measure of this because it is quadratic with permittivity at such high frequencies [25]. However, the index of refraction is a complex number where the imaginary part concerns the optical absorption of the material. In general, solvents are colorless and thus transparent in the visible range, with absorption bands only in the UV and NIR causing anomalous dispersion there. As a consequence, the center of the visible range is far away from such interference and particular suitable for obtaining the real part of the index of refraction. The sodium D emission line at 589 nm was a versatile light source for the determination of the refractive index and proved to be a good choice because it is located approximately in the middle of the visible range, far from the absorption bands mentioned above. The polarization polarity is calculated from the index of refraction n at the wavelengths of the D line by the Lorentz–Lorenz function [25] $(n^2 - 1)/(n^2 + 2)$.

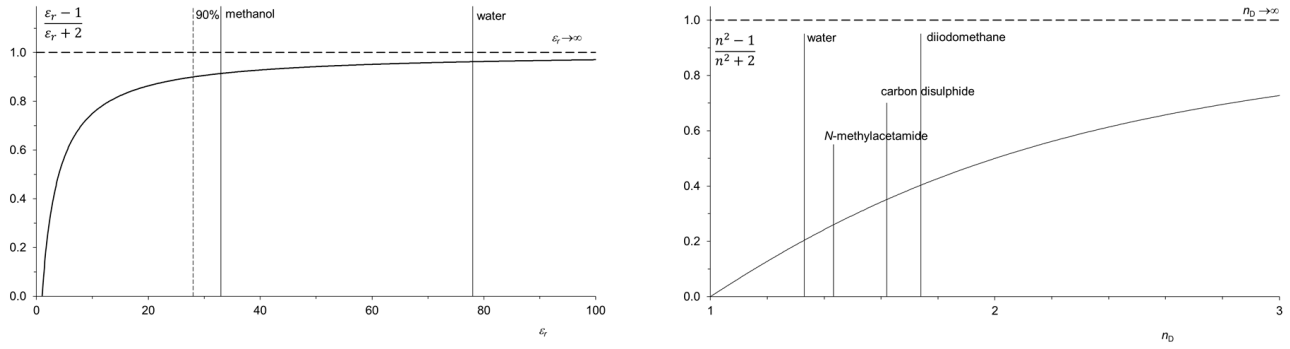

Figure 4. (**Left**) Kirkwood function (vertical axis) as a function of the relative dielectric permittivity ε_r. The dashed vertical line corresponds to 90% of the maximal value of the Kirkwood function [22]. The ε_r values of methanol (33) and water (78) are indicated by vertical lines. (**Right**) The index of refraction n_D as a measure of the polarizability of solvents. The region of n_D of solvents essential for preparative chemistry extends between the values for water (1.33) and diiodomethane (1.74). The values of the highly polarizable carbon disulfide (1.62) as versatile solvent and *N*-methylacetamide (1.43) with high ε_r are marked by vertical lines.

According to the Debye function, solvent polarity by orientation (named dipolarity for short) and by displacement polarization (named polarizability for short) were discussed individually. The use of the relative dielectric permittivity (dielectric constant ε_r; see Figure 4, left) to describe the dipolarity of solvents [26] is not consistent with general chemical experience because of the rapid saturation at which 90% of the effect is achieved for $\varepsilon_r = 28$ (this is even worse in models for ellipsoidal occupancies). Moreover, the appreciable and chemically important difference in chemical solvent polarity between methanol and water is barely reflected in the model, and solvents such as *N*-methylformamide ($\varepsilon_r = 182$) and *N*-methylacetamide ($\varepsilon_r = 191$) would be incorrectly estimated to be even appreciably more polar than water ($\varepsilon_r = 78$). The Lorentz–Lorenz [27] function [28] in Figure 4, right, indicates a comparably narrow range of n_D values relevant for solvents most commonly used in preparative chemistry, between the lower limit given by polar water ($n_D = 1.33$) and the highly polarizable carbon disulfide ($n_D = 1.62$). The upper limit is given by the rarely used solvent diiodomethane ($n_D = 1.74$). Again, water is estimated to be less polar than *N*-methylacetamide ($n_D = 1.43$). Linear combinations between functions of ε_r and n_D did not yield substantial improvement [29–33]. Finally, a theory of dipole swarms was developed [34] but is limited to minor polar solvents. The mentioned discrepancies may be caused by the fact that a macroscopic volume property of a medium is characterization by permittivity, while chemical reactions and solvation are determined by microscopic, molecular effects.

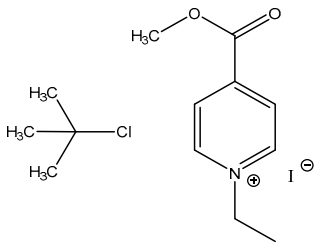

1 **2**

$$lg\,(k/k_{80E}) = m \cdot Y \quad (9)$$

Significant progress was made by using the solvolysis of *tert*-butyl chloride, compound **1**, as a molecular polarity probe by Grunwald, Winstein, and Jones [35–37]. The logarithm of the rate constant k of the unimolecular ionization (S_N1 reaction) of an alkyl halide over the rate constant k_{80E} of the reference reaction of solvolysis of *tert*-butylchloride, compound **1**, in 80% ethanol/water (80E) was set to the product of m as the reaction-characterizing parameter and Y as the solvent-characterizing parameter in Equation (9). This linear free energy relationship (LFE) [38] is equivalent to Hammett's equation [39] for substituent effects. By definition, m becomes one for the solvolysis of *tert*-butylchloride (**1**) and Y becomes zero for the reference 80% ethanol/water (80E). The Y values for solvent polarity correspond well to chemical experience, but the polarity scale is not universal being limited to sufficiently strong ionizing solvents such as alcohols and mixtures of alcohols and water. Substrates more complex than **1** can lead to deviations [40].

$$Z = 28{,}591\ [\text{nm}\cdot\text{kcal}\cdot\text{mol}^{-1}]/\lambda_{max} \quad (10)$$

Kosower introduced [41] the more universal solvatochromic polarity probe **2** in which ionization to generate charge was replaced by the reverse process, the loss of charge by an optically induced charge transfer (see Figure 5). Solvation affects the polar ground state of salt **2** and lowers its energy, while the electrically neutral electronically excited state is only slightly affected by solvent effects, due to the lost charge. The molar energy of electronic excitation of the maximum (λ_{max}) of the CT band of **2** is obtained by Equation (10) and was defined as the Z polarity scale; the dimension is not given in SI units because of the more convenient kcal/mol at the period of publications and is also retained here for

polarity scales to avoid confusion (the energy has to be multiplied by 4.184 kJ·kcal^{-1} to obtain SI units).

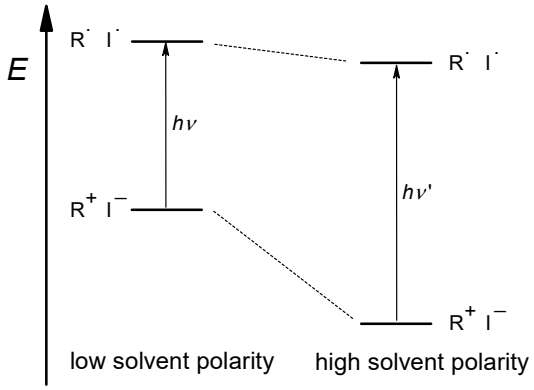

Figure 5. Schematic representation of the solvent effect on the energetic position (E) of dye **2** in the electronic ground and excited states: The energy difference is related to the wavelengths λ of the absorbed light in the CT transition $\Delta E = h\nu = h{\cdot}c/\lambda$.

The Z scale exhibits a linear correlation with the Y scale for various solvents (see inset of Figure 6). This LFE indicates that the same effect is described. The Z-scale brought about an appreciable progress because it is not limited to strongly ionizing solvents (see open circles in Figure 6), but can be extended to solvents with lower polarity (see filled circles in Figure 6). However, polarity probe **2** is still not optimal because (i) the solubility in low-polarity solvents such as hydrocarbons is very low and impedes experimental work, (ii) the CT band is in the hypsochromic visible region and is shifted to the next absorption band for highly polar solvents so that spectral overlap interferes, (iii) the molar absorptivity of **1** is comparably low and requires appreciable concentrations for UV/Vis measurements with standard equipment, and this addition may alter the polarity of the solvent since it is a polar salt.

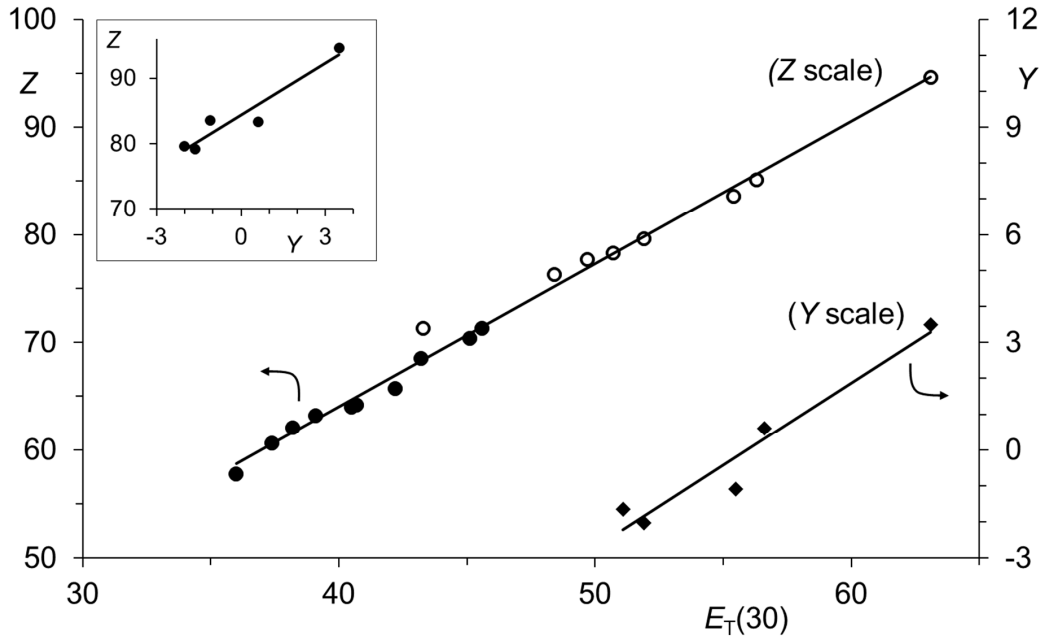

Figure 6. Linear correlation (diamonds) for solvent effects (LFE) between the Y scale (*t*-BuCl **1**) and the $E_T(30)$ scale (compound **3**, right ordinate, correlation number 0.97 with 5 solvents, coefficient of determination 0.94, standard deviation 0.66, slope 0.46, intercept –26; solvents from right to left:

H_2O, $HCONH_2$, CH_3CO_2H, CH_3OH, C_2H_5OH). Linear correlation for the *Z* scale (compound **2**) and the $E_T(30)$ scale (compound **3**, left ordinate, correlation number 0.995 for 18 solvents, coefficient of determination 0.991, standard deviation 1.0, slope 1.33, intercept 11.0; solvents from right to left: (hydrogen-bonding solvents: hollow circles) H_2O, $HOCH_2CH_2OH$, CH_3OH, C_2H_5OH, 2-C_3H_7OH, *n*-C_4H_9-1-OH, 1-C_3H_7OH; (non-hydrogen-bonding solvents: Filled circles) CH_3CN, DMSO, *t*-C_4H_9OH, DMF, $(CH_3)_2CO$, CH_2Cl_2, pyridine, $CHCl_3$, $CH_3OCH_2CH_2OCH_3$, THF, 1,4-dioxane. *Inset:* Linear correlation between the *Y* scale (*t*-C_4H_9Cl **1**) and the *Z* scale (compound **2**, correlation number 0.96 for 5 solvents, coefficient of determination 0.91, standard deviation 2.1, slope 2.6, intercept 84; solvents from right to left: H_2O, $HCONH_2$, CH_3CO_2H, CH_3OH, C_2H_5OH).

4. Pyridinium Phenolate Betaines

Covalent bonding of a negatively charged structural element to the positively charged pyridinium structure in **3** to form a zwitterionic betaine enabled an intramolecular light-induced charge transfer. As a result, substantial improvement was achieved not only by increasing the molar absorptivity, but also by further extending the polarity scales to low-polarity media due to the application of an electrically neutral polarity probe. The dipole moment of a structure with a single bond of an iminium anion to the pyridinium nitrogen atom was still small and resulted in moderate solvatochromism [42] (see further discussion in Refs. [43,44]), whereas with a 4-oxyphenyl anion [45] as the *N*-substituent, the charges were further separated, inducing strong solvatochromism [46]. Dimroth, Reichardt, and coworkers investigated [47] various *N*-4-oxyaryl derivatives for solvatochromism and found optimal properties of the betaine 30 (**3**, B30, CAS RN 10081-39-7), which provided a significant advance.

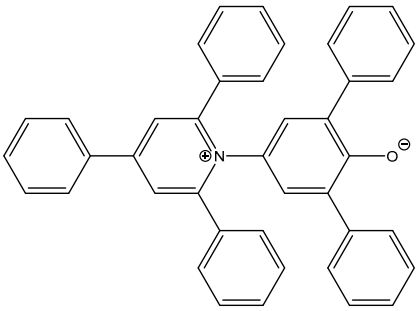

3

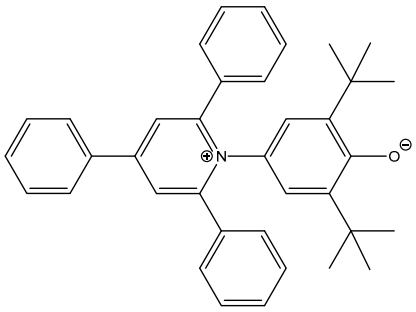

4

Dye **3** is remarkably strongly solvatochromic, so that solutions are yellow in water, red in methanol, violet in ethanol, blue in 1-butanol, green in acetone, and absorb in 1,4-dioxane in the NIR. The molar energy of light absorption at the maximum is called $E_T(30)$ value of a solvent (transfer energy of betaine No. 30 in the first publication) is calculated analogously to *Z* in Equation (11) and are meanwhile determined for almost 400 solvents [48].

$$E_T(30) = 28{,}591\ [\text{nm}\cdot\text{kcal}\cdot\text{mol}^{-1}]/\lambda_{max} \quad (11)$$

The $E_T(30)$ values correlate linearly with the *Y* and *Z* values for various solvents (see Figure 6) and thus describe the same dipolarity effect of solvents. The linear correlation with *Z* values includes lipophilic solvents (filled circles) and polar protic solvents (open circles). The correlation with the Z values is of special importance for solvent effects because hydrogen bonds, as strong non-covalent interactions, are unimportant for the ion pair **2** (HI's remarkably low boiling point of −35.4 °C, in spite of its high molecular weight, can be seen as an indicator of the absence of hydrogen bonds to I (see also the related discussion in ref. [49])). As a consequence, hydrogen bonds for **3** are estimated to be insignificant. Apparently, the five peripheral phenyl groups in **3** shield the betaine to such

an extent that specific solvent effects play a minor role, but still allow the exceptionally strong solvatochromism. Dye **3** is a highly sensitive optical probe for other solvent effects as will be discussed later.

The *tert*-butyl derivative **4** (No. 26 in the first publication [47]) also exhibits very pronounced solvatochromism (E_T(26) values); however, the phenolate oxygen atom does not appear to be as efficiently shielded as in **3**. A good linear correlation is obtained between E_T(30) and E_T(26) values (performance of target to actual comparison) for lipophilic solvents, shown as filled circles and the solid linear regression line in Figure 7. For hydrogen-bonding solvents (open circles and the dashed linear regression line), deviations from this line are observed forming a second linear regression. Obviously, the effect of hydrogen bonding causes a much stronger influence of solvents on the solvatochromic chromophore. The scattering of points within this second correlation is significantly larger than within the first, indicating a stronger contribution of specific solvent effects; such effects were already referred in the first reference to **4** [47].

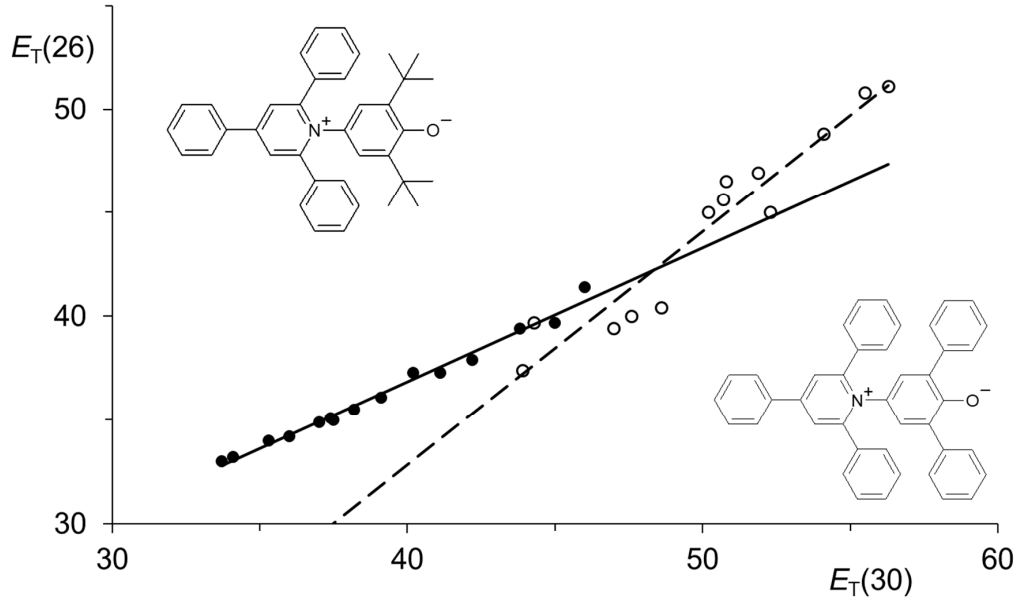

Figure 7. Linear correlation between the E_T(30) (dye **3**) and E_T(26) (dye **4**) values for pure solvents from Ref. [47] the standard deviations are indicated. Filled circles and solid line: non-hydrogen-bonding solvents; slope: 0.64; intercept: 11.5 correlation number 0.993 for 15 solvents, standard deviation 0.30; coefficient of determination 0.987. Open circles and dashed line: Hydrogen-bonding solvents; slope: 1.1; intercept: −12.1; correlation number 0.960 for 13 solvents; standard deviation 1.31; coefficient of determination 0.924. Solvents with increasing E_T(30) values: $C_6H_5CH_3$, C_6H_6, $C_6H_5OC_6H_5$, 1,4-dioxane, 2,6-lutidine, $(CH_2)_4O$, C_6H_5Cl, $CH_3OCH_2CH_2OCH_3$, $CHCl_3$, C_5H_5N, CH_2Cl_2, CH_3COCH_3, $HCON((CH_3)_2$, $(CH_3)_3COH$, $C_6H_5NH_2$, CH_3SOCH_3, CH_3CN, $(CH_3)_2CHCH_2CH_2OH$, 2,6-$(CH_3)_2C_6H_3OH$, $CH_3CHOHCH_3$, $CH_3CH_2CH_2CH_2OH$, $CH_3CH_2CH_2OH$, $C_6H_5CH_2OH$, CH_3CH_2OH, $HOCH_2CH_2OCH_3$, $HCONHCH_3$, CH_3OH, $HOCH_2CH_2OH$.

The solvatochromism of a derivative of **4** without peripheral phenyl groups was studied by Sander and co-workers [50] and showed a linear correlation with E_T^N and E_T(30) values, respectively, for both hydrogen-bonding and non-hydrogen-bonding solvents. This indicates the dominance of dipolarity concerning solvatochromism such as for **3**. The measurements of UV/Vis absorption spectra at low temperature in matrices of solid noble gases at 3 K and slightly higher temperatures such as 25 K gave spectra similar to those expected in the gas phase. The targeted addition of a small amount of water allowed the investigation of its influence and the formation of hydrogen bonds at low temperatures.

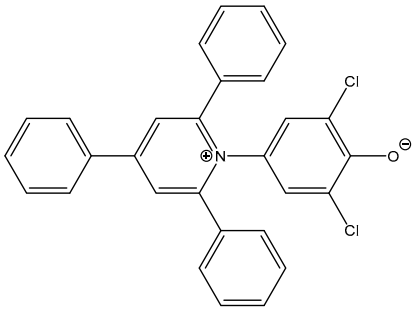

5

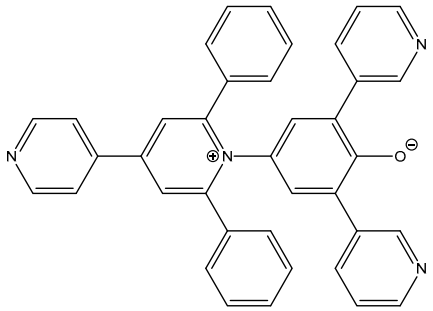

6

The limitations in the application of **3** could be overcome by slightly adapted derivatives. Dye **3** could not applied for acidic solutions such as acetic acid because of the protonation of the basic phenolate anion; Kessler and Wolfbeis [51] developed dye **5** in which the electron depletion by the chlorine atoms lowers the basicity sufficiently to study acidic media, while the solvatochromic behavior is similar to **3** so that extrapolations by linear correlation are possible. Wolfbeis named the polarity values obtained with **5** $E_T(33)$ in continuation of the initial publication by Dimroth, Reichardt, and co-workers. The measurements of highly polar hydrogen bond-forming solvents and solution of salts becomes problematic with **3** because of its low solubility and tendency to aggregate [52]. Reichardt developed dye **6** with the more hydrophilic structure elements of pyridinyl [53] in the periphery of **3**; the *m*-positions of the phenolic aryl substituents in **6** appear to cause minimal interference with solvatochromism, presumably because of the non-conjugation of the phenolate oxygen atom. As a result, the $E_T(30)$ values of many polar and electrolyte-containing solvents can be estimated by extrapolation using **6**.

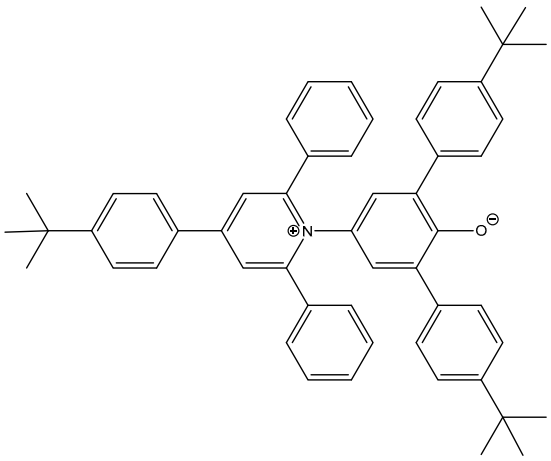

7

The measurement of the $E_T(30)$ values of media with very low dipolarity such as aliphatic hydrocarbons or tetramethylsilane is restricted due to the minimal solubility of the dye. The solubility-increasing effect of *tert*-butyl groups in lipophilic media [54] was applied to dye **7**, whereby a substitution in the periphery allowed an increase in solubility in such media without significantly affecting solvatochromism so that the corresponding $E_T(30)$ values could be obtained by extrapolation by means of a linear free energy relationship [55].

Finally, the experimental $E_T(30)$ values were scaled for easier comparability, first according to Reichardt as a relative polarity measure (*RPM*) [56] where the value for *n*-hexane was set to 0.000 and $RPM = [E_T(30)_{n\text{-hexane}} - E_T(30)_{\text{solvent}}]/E_T(30)_{n\text{-hexane}}$. Next, the scaled $E_T{}^N$ values were defined [57] where the value for tetramethylsilane was set to 0

and for water set to 1, such that $E_T{}^N = [E_T(30)_{solvent} - E_T(30)_{tetrametylsilane}]/[E_T(30)_{water} - E_T(30)_{tetramethylsilane}]$. The experimental $E_T(30)$ values were retained here, although scaling is attractive, because all $E_T{}^N$ values depend on only two references and their accuracy; if their values might be altered, such as by more precise measurements, the entire set of values would change. Moreover, the value for tetramethylsilane is less reliable because it was obtained by extrapolation, and the value for water is at the limit of direct measurements because of the low solubility of **3**. On the other hand, each experimental $E_T(30)$ value has obtained its individual accuracy, which is determined only by the particular experimental procedure, and is considered to be more reliable.

The molar energy of excitation of dye **3** in various solvents as $E_T(30)$ values was taken from the maximum of the solvatochromic band since an efficient and precise measurement is possible. On the other hand, the band can be split [58] into more than a single Gaussian [59] band, and the point of gravity may be of greater physical significance than the maximum because it represents the thermal energy of chromophores. However, accurate determination is more difficult and requires a clear cut between the most bathochromic band and other partially overlapping bands of higher electronic energy, leading to uncertainties. As a consequence, the molar energy of excitation is retained for the following discussions, while trying to avoid over-interpretation.

5. Polarizability: Further Solvent Effects

The concept of estimating solvent polarity on the basis of solvatochromism was developed by Brooker [60] and co-workers based on the study of a large number of merocyanines in early work. He found essentially two branches of solvent effects [61] that appear to be orthogonal to each other, causing blue and red shifts in the absorption spectra as the polarity of the solvent is increased.

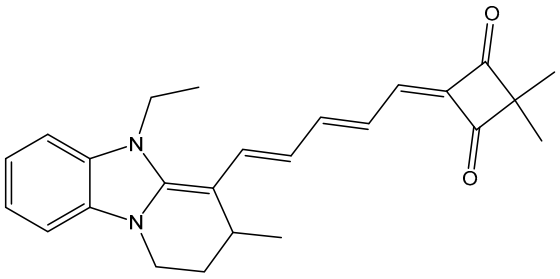

8

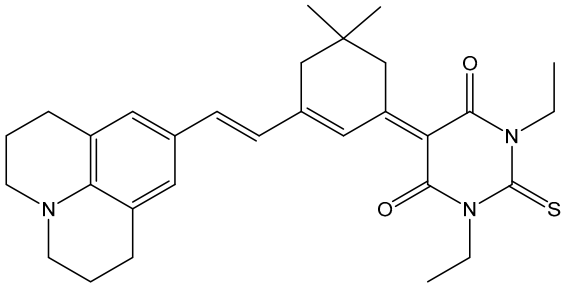

9

The most pronounced blue shift was observed for **8** (RN 3210-95-5) where the polarity scale based on the molar energy of electronic excitation was named χ_B, while a pronounced red shift was found for **9** (RN 2913-22-6), giving the polarity scale χ_R. A linear correlation between the χ_B scale and the Z scale was found for several pure solvents, and there is also a linear correlation between χ_B scale and the $E_T(30)$ scale indicating that the same effect is described, essentially the dipolarity of solvents. Further study of **8** and **9** is hampered by their difficult synthesis; there is only one paper by Brooker (and a patent) referred to for **8** by the *Chem. Abstr.* and six papers for **9**. As a consequence, χ_B is replaced here by a more accessible and similar $E_T(30)$ scale and further discussion is focused to χ_R. The solvent effect in the χ_R scale correlates better [62] with a function of the refractive index of a medium than with dielectric permittivity. As a result, χ_R is mainly better attributed to the polarizability of a medium than its dipolarity. This was further confirmed by finding the missing link [63] between the two polarity scales: χ_B (or, respectively, the $E_T(30)$ scale) and χ_R.

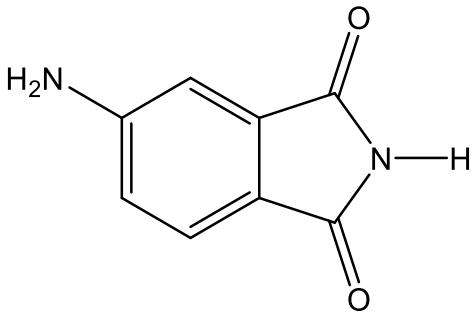

10

The 4-aminophthalimide **10** is solvatochromic in fluorescence and is similar to *N*-methyl-4-aminophthalimide, the fluorescent dye for Zelinski's [64] universal polarity scale *S*.

The molar energy of fluorescence of **10** was defined as the $\sum$ scale for solvent polarity and correlates linearly with the $E_T(30)$ scale for pure solvents (see Figure 8a). The light absorption of **10** is also solvatochromic and was defined as the σ scale for solvent polarity and correlates linearly with the χ_R scale (see Figure 8b). As a consequence, all solvent polarity scales can be interrelated.

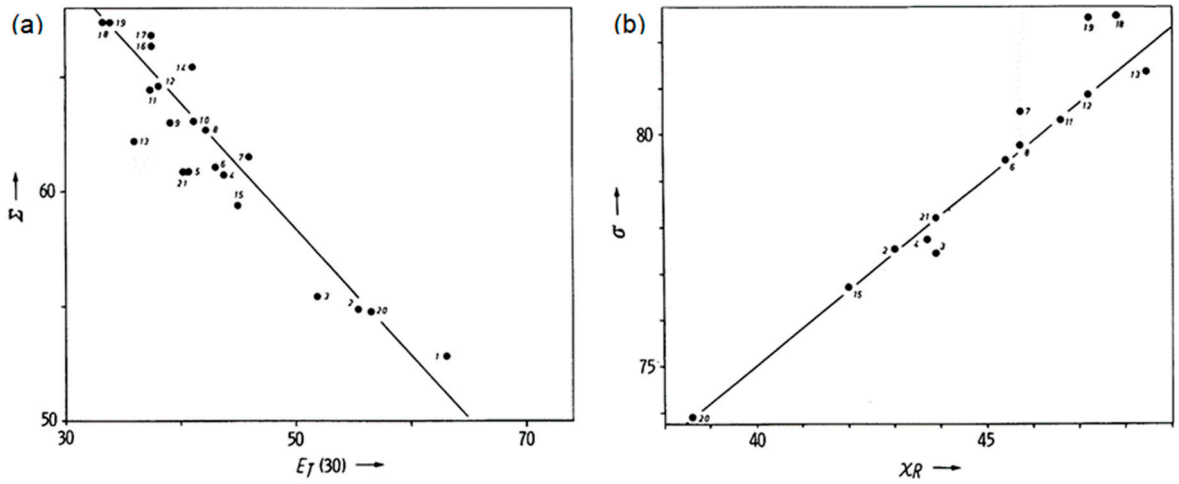

Figure 8. Linear correlation of polarity scales for the pure solvents water (1), methanol (2), ethanol (3), dimethylformamide (DMF, 4), dimethylphthalate (5), butyronitrile (6), acetonitrile (7), acetone (8), chloroform (9), diethylphthalate (10), tetrahydrofurane (THF, 11), ethylacetate (12), 1,4-dioxane (13), dichloromethane (14), dimethylsulfoxide (DMSO, 15), bromobenzene (16), chlorobenzene (17), *m*-xylene (18), toluene (19), formamide (20), and pyridine (21). (**a**) Molar energy of the fluorescence of **10** ($\sum$ scale) versus the $E_T(30)$ scale; (**b**) molar energy of the optical excitation of **10** (σ scale) versus the χ_R scale. The larger scattering of points compared to previous plots is attributed to some contributions of specific solvent interactions.

The correlation in Figure 8b between σ and χ_R is interpreted in terms of the dynamics of light absorption of **10** with a low dipole moment electronic ground state and a much larger dipole moment in the electronically excited state (see Figure 9). The energy of the electronic ground state is only slightly affected by polar solvents. Light-induced electronic excitation increases the dipole moment of **10**; however, solvation by re-orientation of the solvent molecules cannot follow this rapid, essentially vertical process. As a result, the polarizability of the solvent remains important and characterizes the solvent effect on this transition; the same effect is important for χ_R and explains the linear correlation between these two polarity scales shown in Figure 8b. The fluorescent lifetime of the electronically

excited state of **10** in the order of nanoseconds is long enough for relaxation due to the re-orientation of the solvent molecules, and this process is energetically strongly influenced by the dipolarity of the solvent; consequently, a linear correlation of the molar energy of fluorescence ($\sum$ scale) with the $E_T(30)$ scale can be explained because both scales are affected by the same process of solvation. In summary, for the $E_T(30)$ scale, solvation by dipolar re-orientation of the solvents is crucial, while the χ_R scale describes the polarizability of solvents.

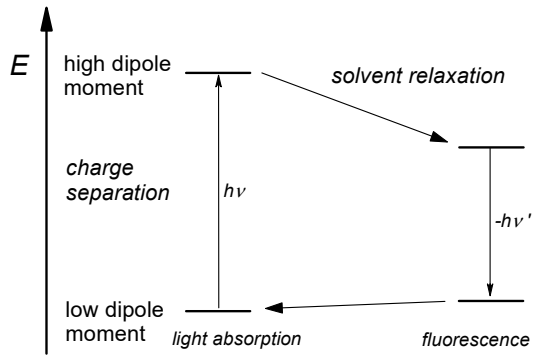

Figure 9. Schematic representation of the solvent effect on the energetic position (E) of dye **10** in the electronic ground and excited state ($\Delta E = h\nu = h{\cdot}c/\lambda$). The electronic excitation of **10** causes a charge separation, with subsequent solvent relaxation affecting the wavelength of fluorescence.

Strong solvatochromic effects of other similar merocyanines were reported [65].

The high dipolarity of water (solvent 1) and aliphatic alcohols is manifested in Figure 8a and corresponds to chemical experience, while the polarizability of these solvents shown in Figure 8b is only in the middle range and is clearly exceeded by solvents such as formamide (20) and DMSO (15).

6. Various Solvent Effects: Multi-Parameter Equations

Two orthogonal solvent properties, the dipolarity and polarizability, have been described above and are the microscopic, molecular counterpart to Debye's equation [23,24] of the linearly independent macroscopic orientation and shift polarization. This may stimulate the search [66] for further types of microscopic solvent effects that are linear independent from each other and thus should describe orthogonal molecular solvent properties. The hydrogen-bonding ability of solvents has already been discussed here with dye **4**. Other solvent properties such as their Lewis acidity and basicity have been the subject of polarity scales such as Gutmann's [67,68] donor and acceptor numbers, hydrogen donor and acceptor numbers, and more [69]. Different and specialized solvent scales are appropriate for different problems. Consequently, the characterization of solvents with a universal parameter set would be attractive. Various approaches were described in the literature, such as those by Kamlet, Taft and Abboud [70], Catalán et al. [71,72], Koppel and Palm [73], and Vitha et al. [74], two examples of which are detailed here.

$$XYZ = XYZ_0 + s\pi^* + a\alpha + b\beta \quad (12)$$

Kamlet, Taft, and Abboud developed the solvatochromic comparison method as multi-parameter fit in which solvent-dependent properties or processes denoted XYZ in Equation (12), such as the $E_T(30)$ scale, depend on solvents for a linear set of parameter products; XYZ_0 is the intercept of such correlations, and s, a, and b are parameters to be individual to the solvent-dependent system. The parameters π^*, α, and β describe characteristic properties of the respective solvent and are tabulated.

The multi-parameter Equation (12) was applied to the $E_T(30)$ and Z polarity scales where the optimal parameters s, a, and b for a linear correlation were calculated by the application of the least squares method (see Figure 10). Acceptable linear correlations

were found; the interpretation of the parameter *a* as a hydrogen-bond-donating property remains problematic, in particular for the *Z* scale. The value is comparably high, although no hydrogen bonds to I^- of **2** are expected.

$$A = A_0 + b\text{SA} + c\text{SB} + d\text{SP} + e\text{SdP} \quad (13)$$

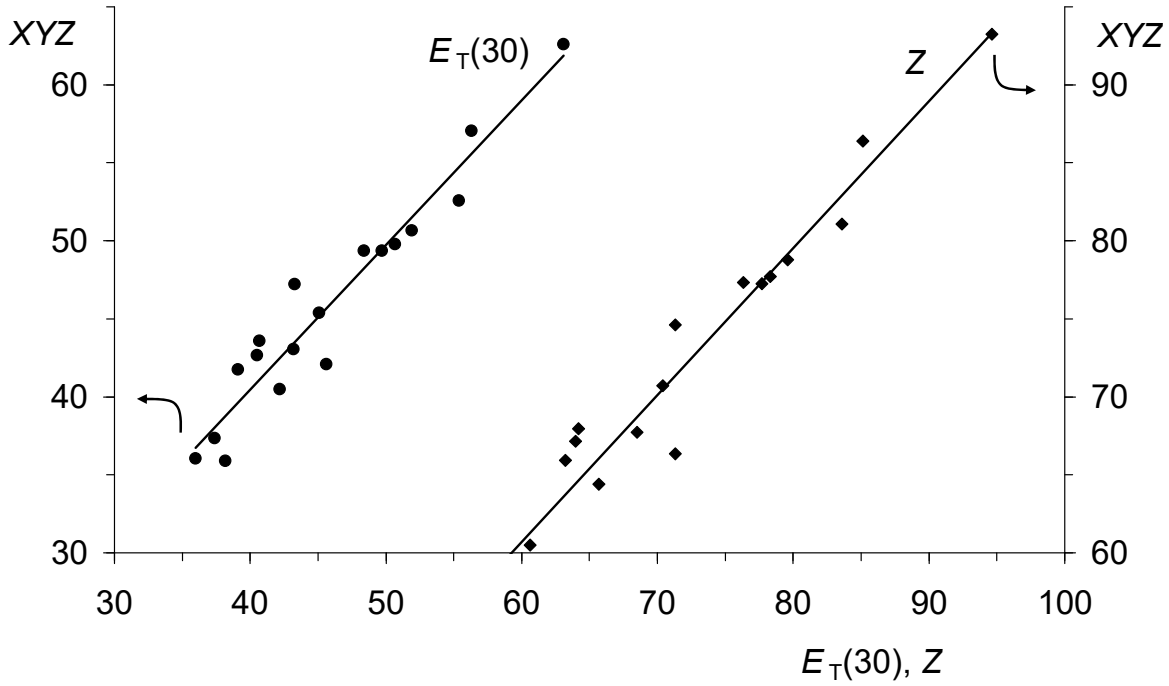

Figure 10. Linear correlations between the $E_T(30)$ and the *Z* scale, respectively, as the abscissa and the adjusted *XYZ* scale of Kamlet and Taft as ordinate. Slope 0.927 for $E_T(30)$ has a correlation number of 0.96 (18 measurements; circles), a standard deviation of 2.0, and a coefficient of determination of 0.93, where the parameters are $s = 16.9$, $a = 15.6$, $b = 4.5$, and $XYZ_0 = 25.1$. Slope 0.943 for *Z* has a correlation number of 0.97 (18 measurements; diamonds), a standard deviation of 2.4, and a measure of determination of 0.94, where the parameters are $s = 20.8$, $a = 21.2$, $b = 7.0$, and $XYZ_0 = 44.6$.

Catalán followed a similar multi-parameter approach with Equation (13), where A describes a solvent-dependent process; *b*, *c*, *d*, and *e* are the process-dependent parameters and A_0 is the intercept of a linear correlation, while the tabulated parameters SdP (dipolarity), SP (polarizability), SA (acidity), and SB (basicity) characterize the medium.

The $E_T(30)$ and *Z* scale were approached by the multi-parameter Equation (13), where the scale-dependent parameter *b*, *c*, *d*, and *e* were determined by the least squares method for 18 solvents (see Figure 11). The correlations were slightly better than in Figure 10; however, an additional parameter was required.

Several improvements to the multi-parameter concept have been developed [75], such as those by Spange [75] and co-workers. Hunter and co-workers [76,77] investigated competing hydrogen-bonding systems as polarity probes. Progress in correlations has been made for individual descriptions of groups of selected solvents; a universal and precise description of solvent effects is still lacking [78]. This may be caused by the interference of residual specific solvent effects with the polarity probes used. Furthermore, the terms of the applied multi-parameter fits might be not fully linearly independent so that cross terms become significant; this may become increasingly important for stronger anisotropic, more ellipsoidal-like solvent molecules where stronger solvent patterning is induced (this might result in liquid crystals) (see also below). As a result, empirical solvent polarity scales and their extension to multi-parameter equations are very useful for practical applications; however, an over-interpretation should be avoided because of their limitations. The size of solvent shells may be of further influence and will be the subject of the next chapter.

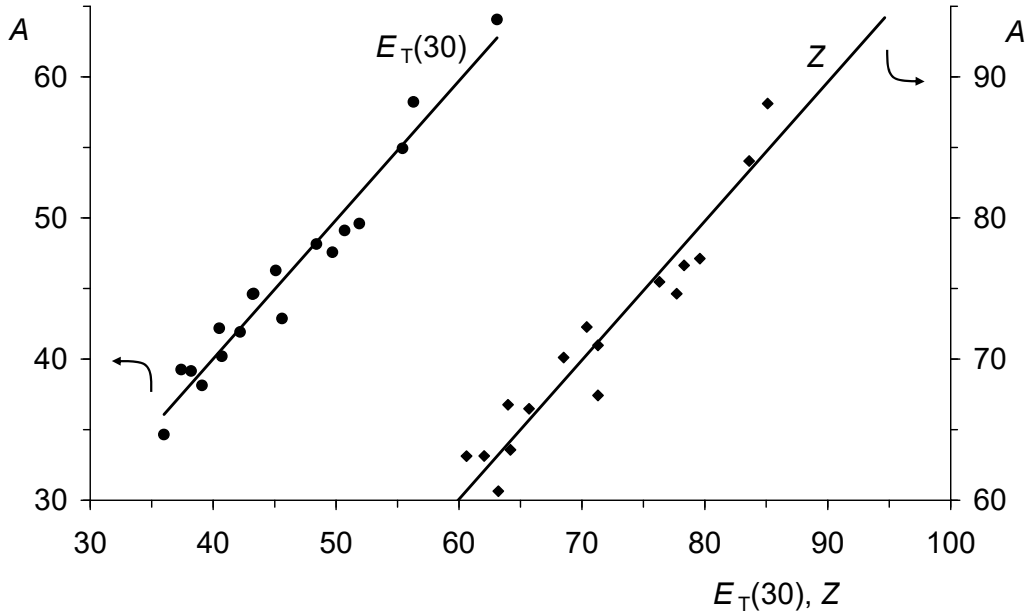

Figure 11. Linear correlations between the $E_T(30)$ and the Z scale, respectively, as the abscissa and the fitted Catalán's A scale as the ordinate. Slope 0.985 for $E_T(30)$ with a correlation number of 0.98 (18 measurements, circles), a standard deviation of 1.6 and a coefficient of determination of 0.96, with parameters are b = 21.4, c = 4.27, d = 5.05, e = 12.7, and A_0 = 25.1. Slope 0.984 for Z with a correlation number of 0.98 (18 measurements. diamonds), a standard deviation of 2.1 and a measure of determination of 0.96 where the parameters are b = 28.6, c = 7.40, d = 5.08, e = 16.6, and A_0 = 44.6.

7. Solvent Shell

Solvated molecules are surrounded by directly molecular interacting solvent molecules; the extension of such interactions into the solvent is of special interest for solvent effects. This topic was investigated using the interaction of strong dipoles with various polar solvent molecules. Betaine B30 (**3**), the solvatochromic probe of the $E_T(30)$ scale, exhibits a comparably large dipole moment of about 12 D [79–82] with a negative charge on the oxygen atom extending into the pyridinium ring with a positive charge. The interaction of the solvent molecules with this dipole moment causes the solvatochromism of **3**. The large and extended electric dipole of **3** generates an electric field that extends into the solvent and can be used as a probe to estimate the extension of a significant solvent shell. For such an assay, two chromophores of **3** were combined [58] *anti*-colinearly to form the dyad **11**.

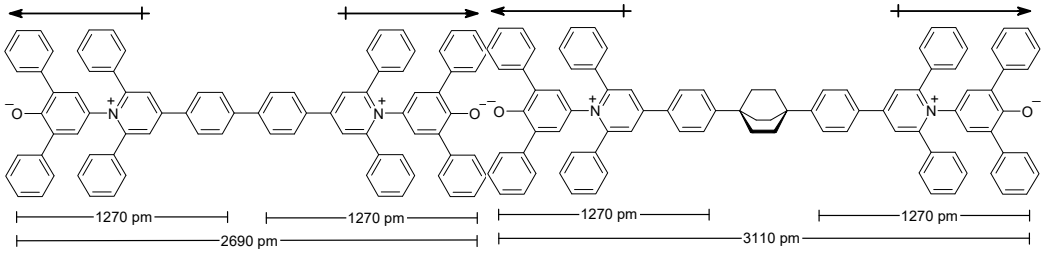

11 **12**

The *anti*-colinearly dipoles in **11** compensate for large distances because no net dipole moment remains so that solvent effects become weak, while at small distances, the effects are still individual and strong so that the solvent effects of each chromophore remain unaffected by the attached second chromophore. The molar energy of excitation of **11** is calculated analogously to **3** and denoted E_T(30dyad).

The solvent effect on the UV/Vis spectra of **3** and **11** is very similar, as is indicated by the linear correlation between $E_T(30)$ and $E_T(30dyad)$ for various solvents (even benzyl alcohol, although an exception, in many cases, is acceptably included) (see Figure 12). The slope of such a correlation can be taken as a measure of the compensation of the dipoles in **11** where a slope of zero should be obtained for complete compensation and a slope of 1 for the absence of any compensation. The slope found experimentally is close to unity, indicating that there is no compensation of the *anti*-collinear dipoles; consequently, the significant solvent shell must be very thin, being not much more than one molecular layer of solvent thick. A possible artifact due to residual conjugation in **11** between the two chromophores could be excluded by using an aliphatic cage in **12** as an isolator; however, **12** gave the same result as **11** [58].

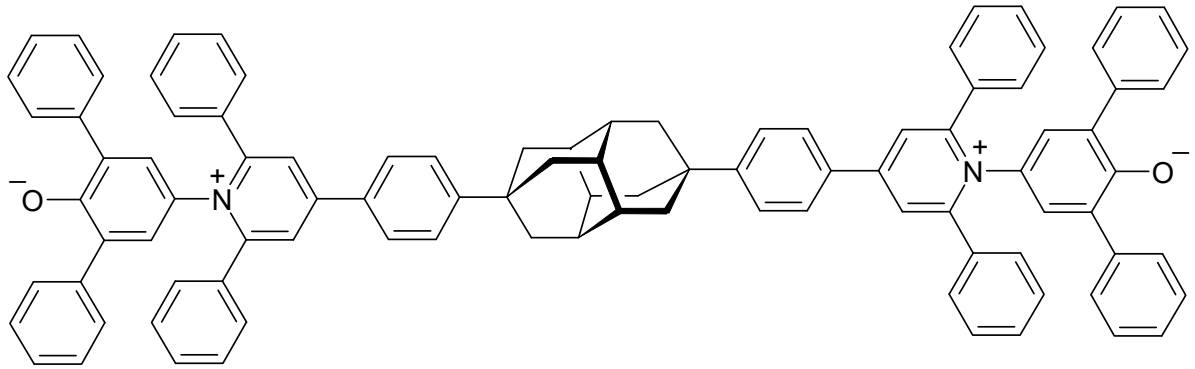

13

Finally, the very rigid diamantane was used as a spacer in **13**. $E_T(30diam)$ as the molar excitation energy of **13** was calculated analogously to **3**.

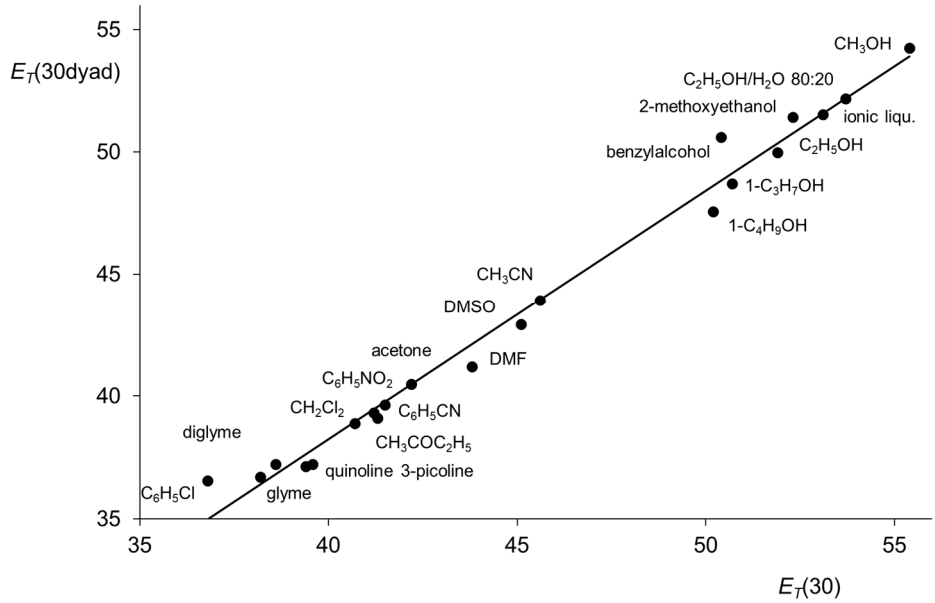

Figure 12. Linear correlation between the $E_T(30)$ values of betaine **3** and $E_T(30dyad)$ values of dyad **11** for various solvents [58] (ionic liqu.: 1-butyl-3-methylimidazolium-tetrafluoroborate). Slope 1.02, intercept −2.43, correlation number 0.993 for 20 points, standard deviation 0.7, coefficient of determination 0.987.

The linear correlation between $E_T(30)$ and $E_T(30diam)$ for various pure solvents is shown in Figure 13; the slope of this correlation of close to unity indicates identical solvent

effects in the $E_T(30)$ and $E_T(30diam)$, thus ruling out significant compensation of the dipoles in **13** with respect to the solvent shell.

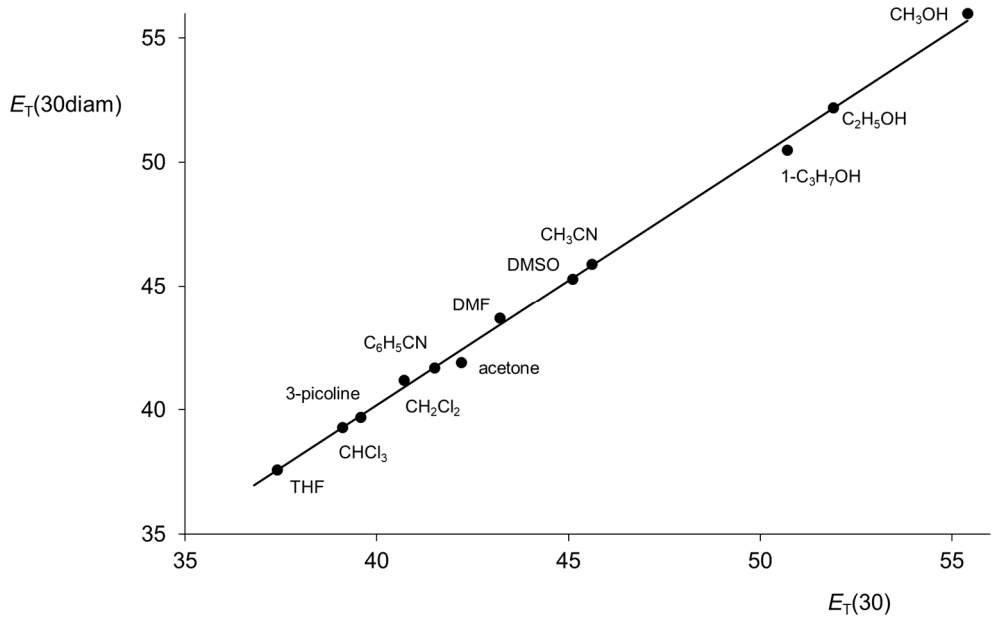

Figure 13. Linear correlation between $E_T(30)$ values of betaine **3** and the $E_T(30diam)$ values of dyad **13** for various solvents [58]. Slope 1.008, intercept −1.33, correlation number 0.9989 for 12 points, standard deviation 0.3, coefficient of determination 0.998.

As a consequence, the solvatochromism of the dyads (**11**, **12** and **13**) based on phenolatebetaine **3** provides no evidence for compensation effects due to *anti*-colinear dipoles and indicates a very thin solvent shell, not much more than one molecular layer thick. The surprisingly thin solvent shell finds its counterpart in the thin surface of liquids such as the phase boundary of water and the gas phase, where investigations [83] indicate an essentially monomolecular active layer, with the hydrogen atoms directed toward the interior of the liquid phase, while the oxygen atoms were found to be in contact with the gas phase. The extraordinarily thin active solvent shell may explain some unaccounted solvent effects such as problems with the relative permittivity (dielectric constant) as a measure of solvent polarity due to some appreciable exceeding of water (see above) although water exhibits a higher polarity according to the chemical experience: The relative permittivity is a three-dimensional property of the volume of a liquid as it is for the refractive index, whereas solvent effects involve two-dimensional molecular surface effects. These can be similar; however, they need not to be identical.

8. Liquid Mixtures

Liquid mixtures are of particular interest for chemists and physicist because the properties of one component can be continuously transformed into the other by changing the composition. Polar molecules in a solvent are surrounded by solvent molecules in diluted solutions and move free of forces in the solvent because the outer sphere corresponds to the solvent. Energy and properties are independent from the positions of the polar molecules such as molecules in the gas phase at low pressure. As a consequence, the same formalism described in Section 2 for gases can be applied to polar additives to solvents: The effect p of the polar component at low concentration is expected to be proportional to its concentration c ($dp = const_1 \cdot dc$) (see also Equation (1)). However, at higher concentrations, this component is expected to interact with itself reducing the effect ($dp = E/c \cdot dc$), where the constant E is a measure of the energetic interaction (see also Equation (2)). The next steps according to Section 2, combination and integration, result in Equation (5). Neither the nature of interaction of the polar component with the solvent nor the interaction with

itself was specified. As a consequence, Equation (5) is to be experimentally verified for its application in binary liquid mixtures; p was set equal to $E_T(30)$ so that Equation (14) is obtained where c^* is the concentration of the polar component at which the interaction of the polar component becomes important and $E_T(30)_0$ is the $E_T(30)$ value of the pure component of lower polarity.

$$E_T(30) = E \cdot \ln\left(\frac{c}{c*} + 1\right) + E_T(30)_o \quad (14)$$

Further approaches [84,85] to the polarity of binary mixtures were reported in the literature.

The validity of Equation (14) for real systems was tested (performance of target to actual comparison) with the mixture *N-tert*-butylformamide/benzene for the $E_T(30)$ polarity scale; a *tert*-butyl group was attached to the formamide to increase the solubility [86] in the aromatic hydrocarbon benzene and to be able to set a broad polarity range. A strongly curved relationship was obtained between the $E_T(30)$ values and the concentration c of the more polar *N-tert*-butylformamide as is shown in the inset of Figure 14. The entire range of concentration c, spanning three decades, could be linearized by Equation (14) (see Figure 14). The strong curvature in the inset is a consequence of the comparably low c^* value of 0.0167 mol·L^{-1}.

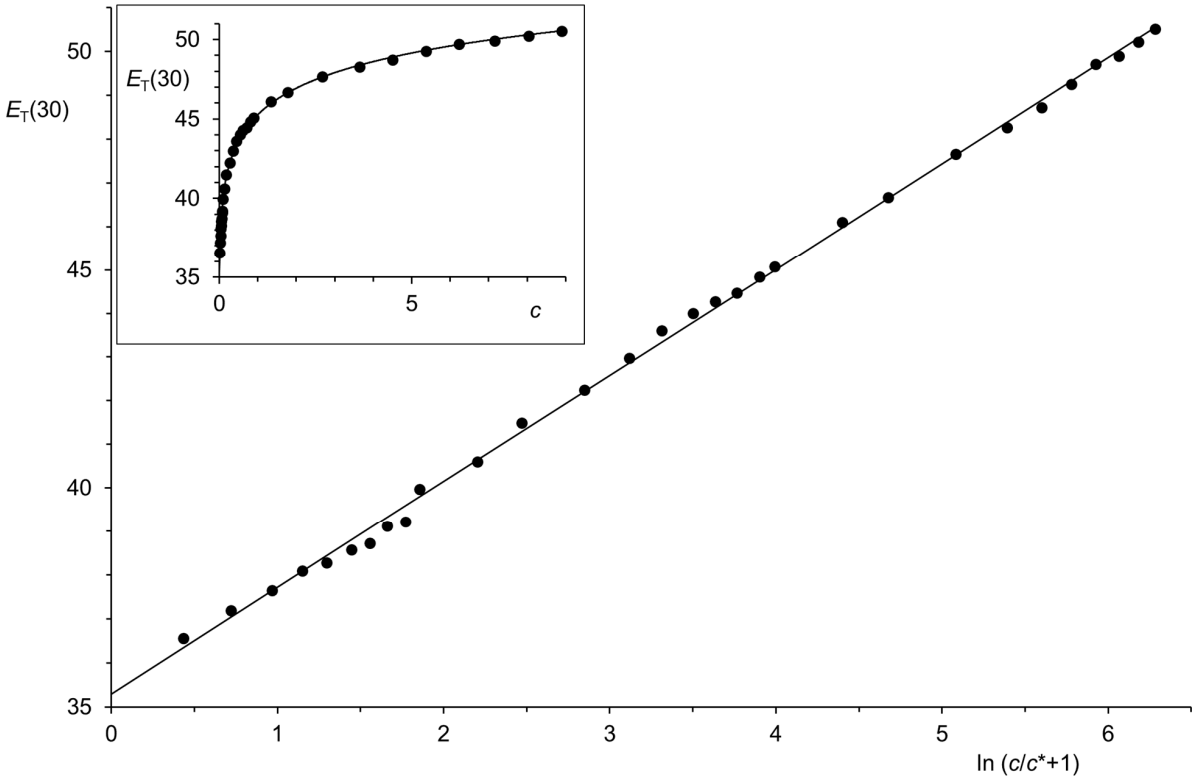

Figure 14. Linear correlation between the $E_T(30)$ values of the mixture *N-tert*-butylforma mide/benzene [87] and ln (c/c^* +1) where c is the molar concentration of the former and c^* = 0.0167 mol·L^{-1}; slope E = 2.43 kcal·mol^{-1}, intercept $E_T(30)_0$ = 35.3 kcal·mol^{-1}, correlation number r = 0.9993, coefficient of determination r^2 = 0.999, standard deviation σ = 0.17 kcal·mol^{-1}. Inset: $E_T(30)$ values of the mixture *N-tert*-butylformamide/benzene as a function of the concentration c in mol·L^{-1} of the former: Measured $E_T(30)$ values (filled circles) and the calculated with Equation (14) (solid curve).

The description of real binary liquid systems using Equation (5) is not limited to the $E_T(30)$ polarity scale, but is more universal [87], as shown by its application to common polarity scales in Figure 15. The validity of Equation (5) has been demonstrated for more than 80 binary mixtures. On the other hand, Equation (5) and Equation (14), respectively, can be used to investigate special properties of liquid mixtures. This will be shown in the next chapter on hydrogen-bonding solvents.

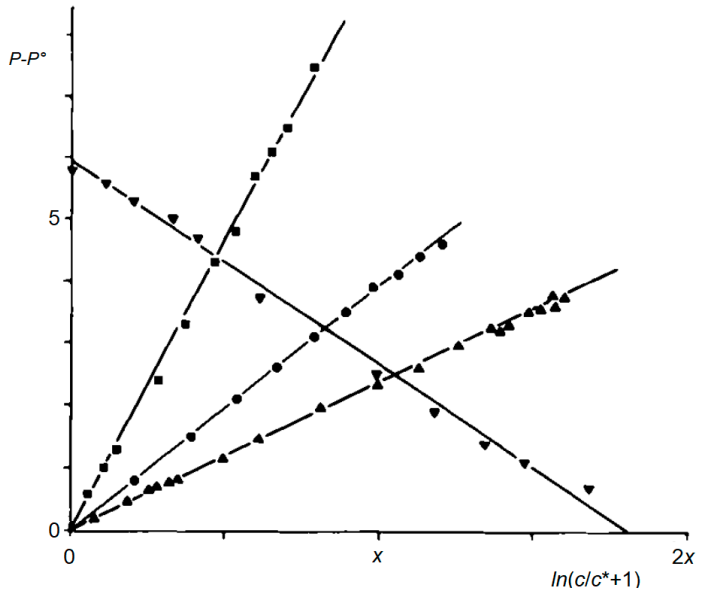

Figure 15. Linear relationship between P and $ln\ (c/c^* + 1)$ for various polarity scales according to Equation (5). Diamonds: $P = E_T(30)$ (methanol/acetone); $x = 2$. Circles: $P = Y$ (water/methanol); $x = 1$. Squares: $P = Z$ (methanol/acetone); $x = 2$. Triangles: $P = \pi_1^*$ (ethanol/*n*-heptane); $x = 1$, ordinate: $P - P^\circ + 5.9$.

9. Hydrogen-Bonding Solvents

Particular attention should be paid to hydrogen bond-forming solvents since hydrogen bonds are strong and directed non-covalent molecular interactions. Therefore, patterning of solvents can be performed by such bonds. On the other hand, the lifetime of hydrogen bonds at room temperature is very short and is in the order of picoseconds [88]. However, the bonds are re-formed in a similarly short period of time, so that molecular sticking structures in the liquid are highly dynamic and enable fast exchange processes. Water, as the most prominent strong hydrogen bond donor is studied here because its low molecular weight allows it to reach the high molar concentration of 55.4 mol·L^{-1}. Water is combined with 1,4-dioxane as a moderate and low-polar hydrogen bond acceptor, where complete miscibility is crucial.

The $E_T(30)$ values of water/1,4-dioxane mixtures as a function of the concentration c of water are shown in Figure 16. Their linear correlation between $ln\ (c/c^* + 1)$ is obtained for concentrations c below 26 mol·L^{-1} as a critical concentration c_k (Figure 16, left line); this correlation corresponds to Figure 14. At higher concentrations, $c > 26$ mol·L^{-1} ($c > c_k$), a second steeper correlation results (the c^* values are low and similar so that the two lines can be combined in one diagram). This sudden change is already obvious in a simple logarithmic plot because of the low values of c^* in both correlations ($ln\ (c/c^* + 1) \approx ln\ c$ for $c >> c^*$); see also the inset top left of Figure 16. The change in slope proceeds in a narrow concentration range and is attributed to a change in solvent structure and corresponds to such a condensation-like phase transition as described for carbon dioxide in Section 2. The formation of the hydrogen-bonded structure requires a sufficiently high concentration to overcome the dissociation at lower concentrations. On the other hand, one can extrapolate the correlation on the left side to higher concentrations until the concentration of pure water

(dashed line) and obtain an $E_T(30)$ value of 55.9. This value would be expected if water did not form a hydrogen bonding structure, and the difference from the actual value of 61 out of 5 units indicates the appreciable increase in solvent polarity due to the formation of the hydrogen-bonded structure.

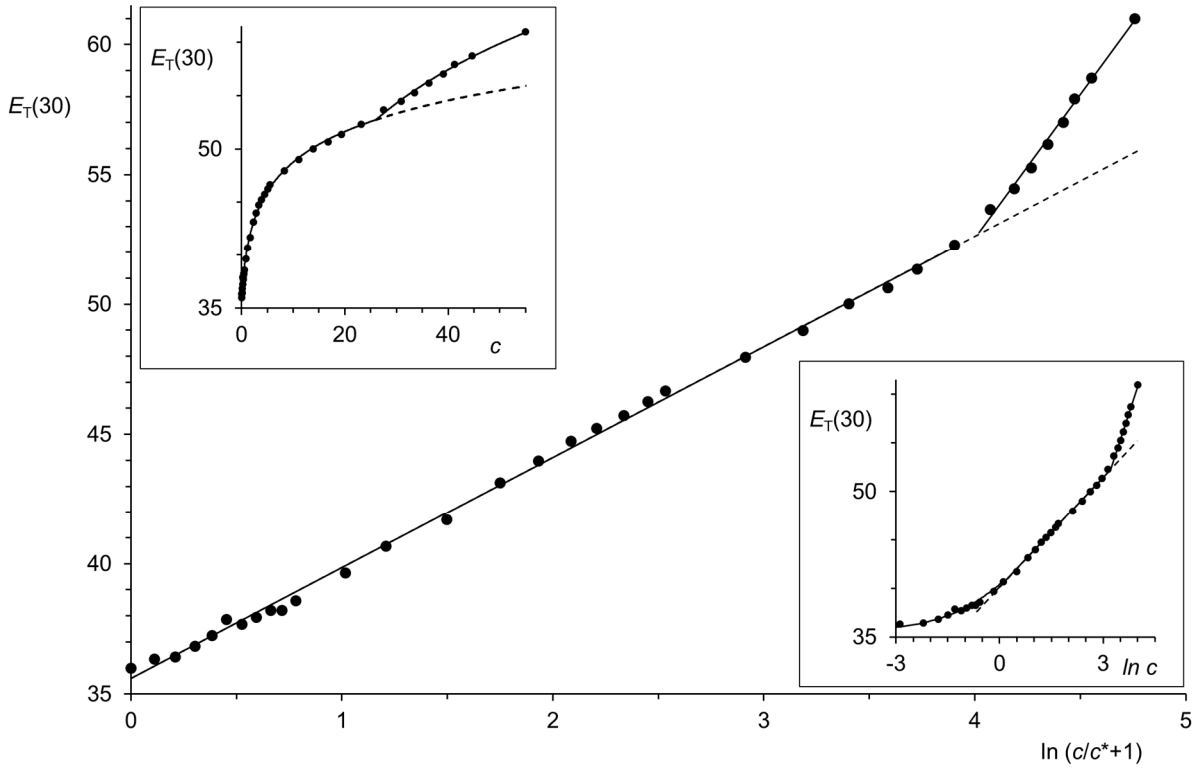

Figure 16. Linear correlation between *ln* (c/c^* + 1) and the $E_T(30)$ values of the mixture water/1.4-dioxane [87] (c^* = 0.48 mol·L^{-1}; measured values as filled circles; linear correlations as lines) as a function of the concentration c of water. Left correlation: E = 4.27, intercept 35.6, standard deviation 0.2, correlation number r = 0.9992 for 27 measurements, measure of determination r^2 = 0.998, extrapolation with the dashed line. Right correlation: E = 11.1, intercept 8.26, standard deviation 0.2, correlation number r = 0.997 for 8 measurements, measure of determination r^2 = 0.993. Inset top left: $E_T(30)$ values of the water/1,4-dioxane mixture as a function of the water concentration c, curves for calculated $E_T(30)$ values, dashed curve for extrapolation. Inset bottom right: $E_T(30)$ values of water/1,4-dioxane as a function of *ln c*; The two linear correlations are already obvious in a simple logarithmic plot because of the low values of c^*.

The formation of double linear correlations according to Equation (5) is neither limited to the $E_T(30)$ polarity scale nor to the mixture water/1,4-dioxane, as can be seen in Figure 17 [89]. Remarkably, the critical concentrations c_k for the transition from one linear correlation to the second are independent of the applied polarity scale within the limits of experimental error and are therefore attributed to a property of water (the kink appears at different position in Figure 17 due to the different scales in the coordinate system). It can surmise that water forms clathrate-like [90] structures at sufficiently high concentrations; however, these structures are very dynamic, unlike the crystalline clathrates such as the hydrate of methane.

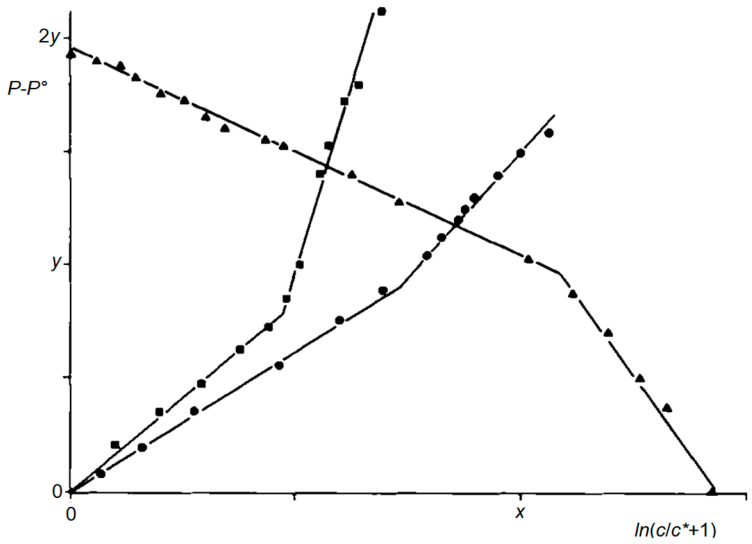

Figure 17. Double linear correlations according to Equation (5) for the water/ethanol mixture and different polarity scales. Filled circles: $P = Y$ ($x = 2$, $y = 1$); filled squares: $P = E_T(1)$ ($x = 1$, $y = 4$); filled triangles: $P = \pi_1^* - 7.7$ ($x = 1$, $y = 4$).

10. Elevation of Polarity

As shown in the last chapter, hydrogen bonds can significantly increase the polarity of the solvent. Consequently, a combination of a moderately polar hydrogen bond donor and a less polar but strong acceptor should increase the solvent polarity.

Ways to increase solvent polarity were tested [91] using the $E_T(30)$ polarity scale and the mixture 1-butanol as the more polar component and hydrogen bond donor and nitromethane as the less polar component and hydrogen bond acceptor. The $E_T(30)$ values of such mixtures as a function of the molar concentration c of 1-butanol pass through a maximum at $c_k = 3.3$ mol·L^{-1} and decrease again to reach the lower $E_T(30)$ value of pure 1-butanol (see Figure 18). The polarity at c_k exceeds the polarity of pure 1-butanol by about 1.6 $E_T(30)$ units. Such an excess of the solvent polarity is interpreted by the formation of a hydrogen-bridged association [91] between 1-butanol as the hydrogen bond donor and nitromethane as the hydrogen bond acceptor, such an associate being more polar than the individual components and means the polar component in Figure 18a bottom right (of course, the molar concentration of this associate is identical with the concentration of 1-butanol because of the 1:1 association). This means that all 1-butanol is captured to form this associate until not enough residual nitromethane is present with increasing concentrations of 1-butanol. Then, a mixture of this associate as the more polar component is formed with 1-butanol so that the polarity of the mixture decreases again because no further associate can be formed. The linear relation between $E_T(30)$ and c_u, the molar concentration of nitromethane, in Figure 18b top right, further supports this interpretation because, according to Equation (5), the polarity increases by the formation of the hydrogen-bonded associate in the medium 1-butanol until all nitromethane is captured in the hydrogen-bonded associate and decreases again to finally reach the lower polarity of pure 1-butanol.

Such mixtures of hydrogen bond donors and acceptors are of particular interest [92] because they offer the possibility to preparing highly polar solvents from components of lower polarity. On the other hand, such mixture exhibits many properties of polar alcohols due to the possibility of rapid intermolecular proton exchange. A completely novel type of polar protic media can be constructed by using chloroform [93] since this solvent exhibits the tendency to form hydrogen bonds to strong hydrogen bond acceptors such as the dipolar aprotic solvents; however, unlike the alcohols, chloroform does not exhibit the tendency to exchange protons under neutral conditions. As a result, comparably polar

protic solvents could be constructed without protons exchange. This might be of interest for various reasons.

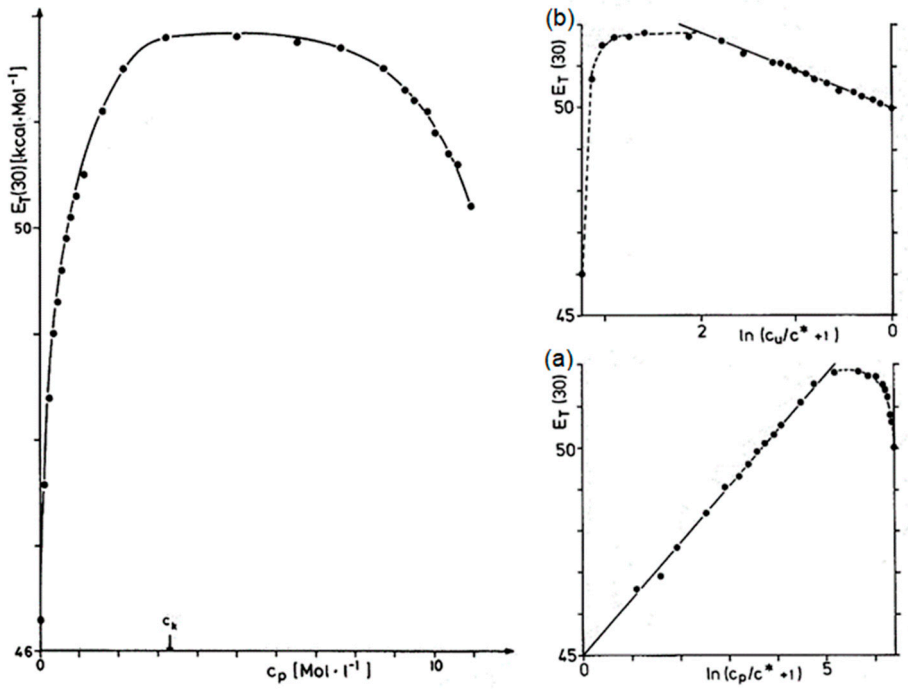

Figure 18. $E_T(30)$ values of mixtures of 1-butanol/nitromethane [91]. (**Left**) $E_T(30)$ values of the mixture nitromethane/1-butanol as a function of the molar concentration c_p of 1-butanol; the maximum is exceeded at c_k = 3.3 mol·L^{-1}. (**Bottom right** (**a**)): Linear correlation between $E_T(30)$ and ln (c_p/c^* + 1) with c_p as the molar concentration of 1-butanol as the solid line and deviations to lower values after passing c_k shown as dashed curve; (**Top right** (**b**)): Linear correlation between $E_T(30)$ and ln (c_u/c^* + 1) with c_u as the molar concentration of nitromethane as solid line and deviations to lower values after passing c_k shown as dashed curve.

11. Polarity around Miscibility Gaps

Homogeneous binary mixtures of very different polar solvents are possible such as 1,4-dioxane ($E_T(30)$ of 36.0) and water ($E_T(30)$ of 63.1), and one solvent in such mixtures can be used as a solubilizer for applications in complex mixtures. In most of such cases, the solubility of each solvent in the other is limited with the miscibility gap determined by the surface energy (surface tension) between both solvents.

The $E_T(30)$ values of methanol/water mixtures as a function of the molar concentration c_p of water can be described by Equation (5) and form two linear correlations as shown in Figure 19 (squares above) [94]; a change in the solvent structure at high water content forms a kink as shown in Figure 16. The same type of double correlation is found for ethanol/water mixtures (triangles down) with a kink at about the same water concentration as for methanol/water (although at a different position on the abscissa because of the different scaling). The mixture of 1-propanol/water (triangles up) is a further example of this behavior starting with a lower $E_T(30)$ value due to the lower polarity of 1-propanol. A miscibility gap is observed for 1-butanol/water (circles). However, similar linear correlations are found [95] in both the low water content range and high water content range where the expected kink is in the miscibility gap (biphasic region) and can be obtained by extrapolation. The similarity between the mixtures of 1-butanol/water and mixtures of lower alcohols indicate that the two types of solvent structure are miscible for the lower alcohols, but no longer completely for 1-butanol. This behavior, dominated by the solvent structure, seems to be more general.

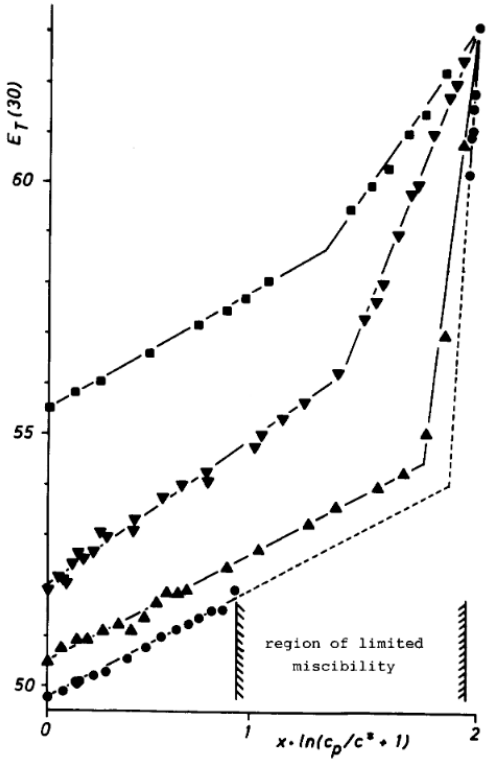

Figure 19. $E_T(30)$ values of binary mixtures between *n*-alkanols and water as a function of ln $(c_p/c^* + 1)$ according to Equation (5) with c_p as the concentration of the polar water [94]; the ordinate was scaled by x to obtain a uniform value for water. Squares: water/methanol (x = 0.157); some values are taken from ref. [47]. Triangles down: water/ethanol (x = 0.318); some values are taken from ref. [47]. Triangles up: water/1-propanol (x = 1.349). Circles: water/l-butanol (x = 1.705). Solid lines result from application of Equation (5) and least squares method; dashed lines are extrapolations into the region of limited miscibility.

12. Polar Functional Groups

The generality of Equation (5) for the polarity of the solvent naturally implies the domination of the polar component in the binary mixture, while the component with lower polarity essentially forms the matrix. The polarity of the more polar component is essentially generated by polar functional groups; as a consequence, the molar concentration of these polar groups should be of fundamental importance.

To verify this concept, the molar concentration of pure alcohols and water was calculated from their density and molecular weight and is identical to the molar concentration of their polar OH group. Plotting the $E_T(30)$ values against their logarithmic concentration in Figure 20 (left) shows a linear relation for 1-propanol (3) and higher homologues [96]. A second steeper line is found for methanol (1) and water (0) indicating the hydrogen-bridging structure of these solvents. Interestingly, the $E_T(30)$ value of ethanol (2) is close to the limit, indicating the special properties of ethanol as a solvent since the hydrogen-bridging structure is just being realized, while slight perturbance such as an increase in temperature or the addition of another component could change the structure to more isolated OH groups with different solvent properties. $E_T(30)$ values for the molar concentrations (*ln* c_p) of OH groups in mixtures of ethanol with the less polar 1,4-dioxane or *n*-heptane fit well into the plot for pure 1-alkanoles, as shown in Figure 20 (right). It can be concluded that the polarity of solvents and solvent mixtures, respectively, is dominated by polar functional groups (polar structure elements) and structures or components with lower polarity essentially form the matrix. This concept was further extended and generalized by Spange and co-workers [97].

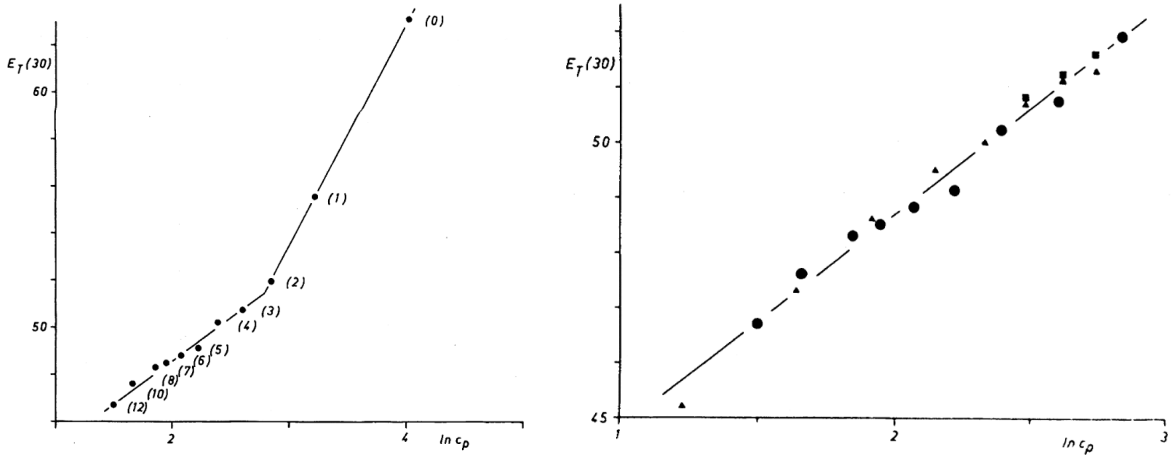

Figure 20. (**Left**) $E_T(30)$ values [56] of homologous linear 1-alkanols as a function of the logarithm of their molar concentration c_p. Their chain lengths n are given in parenthesis such as (0) for water and (1) for methanol. (**Right**) Comparison of $E_T(30)$ values as a function of the logarithm of the molar concentration of OH groups (range of low concentrations of OH groups). Circles: Pure linear 1-alkanols, triangles: Mixtures of ethanol and 1,4-dioxane, squares: Mixtures of ethanol and *n*-heptane.

The piezochromism of **3**, the pressure-dependent shift in the solvatochromic band, may be a further indicator of the importance of the molar concentration of OH groups for the polarity of the medium. An increase in the pressure [98] from atmospheric pressure to 2000 at shifts the solvatochromic band of **3** in ethanol until $E_T(30)$ = 52.7 where the compressibility of ethanol increases the molar concentration from 17.1 to 24.6 mol/L. Such an increase in the concentration of OH groups could be made responsible for the observed increase in the $E_T(30)$ values because the values are within the scope of the second linear correlation in Figure 20.

13. Thermochromism

Most investigations about solvent effects were realized at room temperature or slightly above because of experimental convenience; however, solvent effects are appreciably temperature-dependent. Pronounced effects can be expected for hydrogen-bonding solvents, since such bonds dominate at lower temperatures and become more and more loose at higher temperatures (compare, for example, the high specific heat of water).

The thermochromism of **3** in ethanol [99] is shown in Figure 21, where there is a precise linear relation between the temperature T and the polarity of the solvent as the $E_T(30)$ values. As indicated before, the $E_T(30)$ value of ethanol at room temperature is appreciably lower than of methanol; however, cooling to −75 °C increases the value so that it overtakes even methanol. The thermal expansion of ethanol [100] may be partially responsible for the effect (see, for example, Figure 20 for the effect of the content of OH groups in alcohols); this expansion is exactly proportional to temperature (compare the use in alcohol thermometers); however, one can estimate that the thermal expansion can only cover about 1/3 of the effect. The residual 2/3 is attributed to the loosening of hydrogen bonds by increasing the temperature. Remarkably, this must also be exactly linearly temperature-dependent because the high precision of the overall linear correlation.

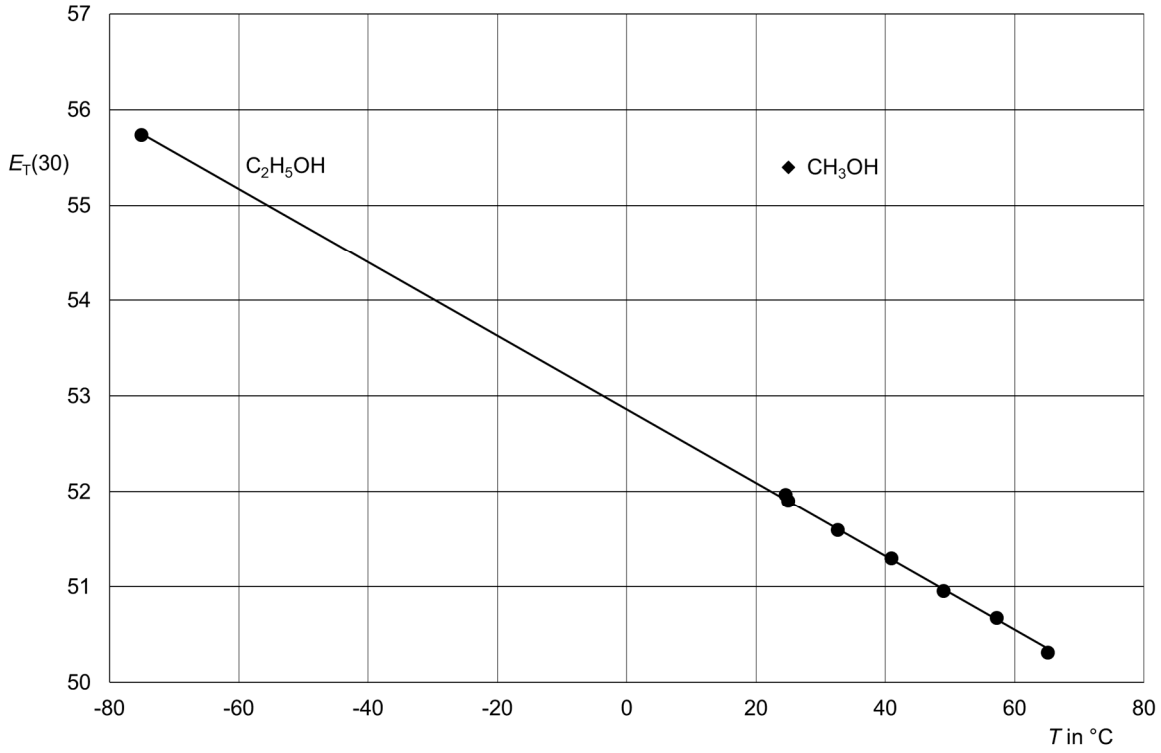

Figure 21. Thermochromism of **3** in ethanol: Filled circles for the measurements (measurements were taken from ref. [99]) and a filled diamond for the polarity of methanol at room temperature for comparison. Linear correlation between T and $E_T(30)$: slope −0.0385, intercept 52.859, correlation number −0.99988 (7 measurements), coefficient of determination 0.9998, standard deviation 0.03.

14. Long-Reaching Noncovalent Interactions

Intermolecular interactions are important for solvent effects where direct molecular contacts appear to dominate; such interactions are strongly damped and become vanishing beyond the direct molecular contact. Longer distances are covered by dipole–dipole interactions such as those according to Förster's mechanism [101,102], where a limit of interactions seems to be reached at more than 10 nm.

However, studies of the concentration dependence of the fluorescence lifetimes τ of strongly fluorescent dyes in Figure 22 indicate [4,103] that there are still interactions even at more than 100 nm because of the large intermolecular distance. Equation (5) was developed without restriction on the nature of interactions. Consequently, the equation can be also used to describe the concentration dependence of τ; see the inset of Figure 22.

The long-reaching interactions were attributed to the effect of evanescent waves of the electronically excited dye molecules. Electronical excitation requires comparably high energy input and is unimportant at room temperature. On the other hand, molecules are vibronically excited even at room temperature. As a consequence, such interactions might be part of solvent effects where an even further reaching can be expected due to the long wavelengths of vibronic energy. This could be the subject of further investigations.

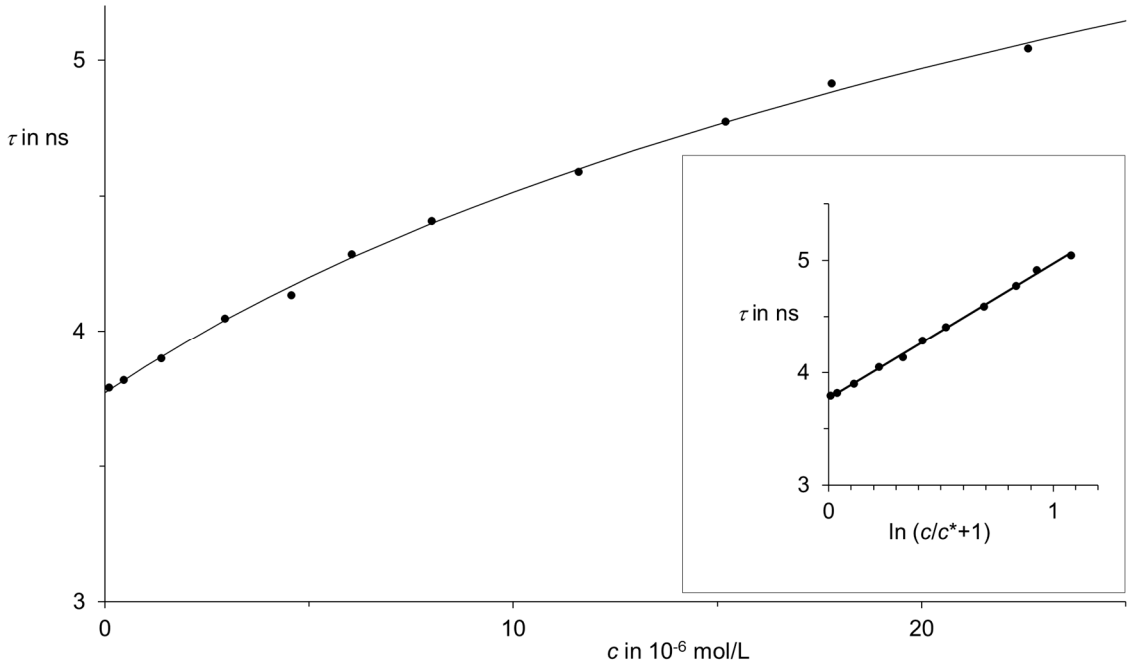

Figure 22. Dependence of the fluorescence lifetime τ on concentration c of highly diluted solutions of the fluorescence dye S-13 (RN 110590-84-6) in chloroform: Measurements as filled circles; curve calculated by means of Equation (5). Inset: linear correlation between τ and $(ln\ c/c^* + 1)$ according to Equation (5): E = 1.199; c^* = $1.17 \cdot 10^{-5}$ mol/L; correlation number 0.9992 (11 measurements); coefficient of determination 0.998; standard deviation 0.02.

15. Practical Applications

The visual effect in the solvatochromism of dye **3** facilitates its application in simple color tests. In anhydrous solvents or reagents, residual contents of water can be determined because these induce strong solvatochromic effects. For example, anhydrous *tert*-butylhydroperoxide is required for various applications in preparative chemistry and forms pure blue solutions [104] of **3**. A low and unimportant water content shifts the color so that it is no longer pure blue, but acquires a very slight violet component, while a higher water content shifts the color to violet and further to red. A simple color test with **3** allows the rapid identification of solvents, as shown for disinfectants [105] and their components. It can also be used to determine the efficiency of methods for drying solvents, in particular, highly hygroscopic solvents such as ethanol. The measurement of the absorption maximum of dye **3** and application of Equation (5) allows the accurate determination of the composition [106] of binary mixture, in particular, the water content [107] of solvents. The use of solvatochromic fluorescent dyes [108] means an extension because higher diluted solutions can be applied and the optical quality of a sample is of minor importance.

Equation (5) was developed for general intermolecular interactions without specifying their nature or method of detection. As a consequence, a linear correlation according to Equation (5) was obtained for the densities [109] of mixture between various solvents and water such as is shown in Figure 23 (left for water/methanol). Similar linear correlations were obtained for the index of refraction corrected by the density ($n_D{}^{20}/\rho$), as shown in Figure 23 (right). Such correlations are useful for various applications such as precise interpolations.

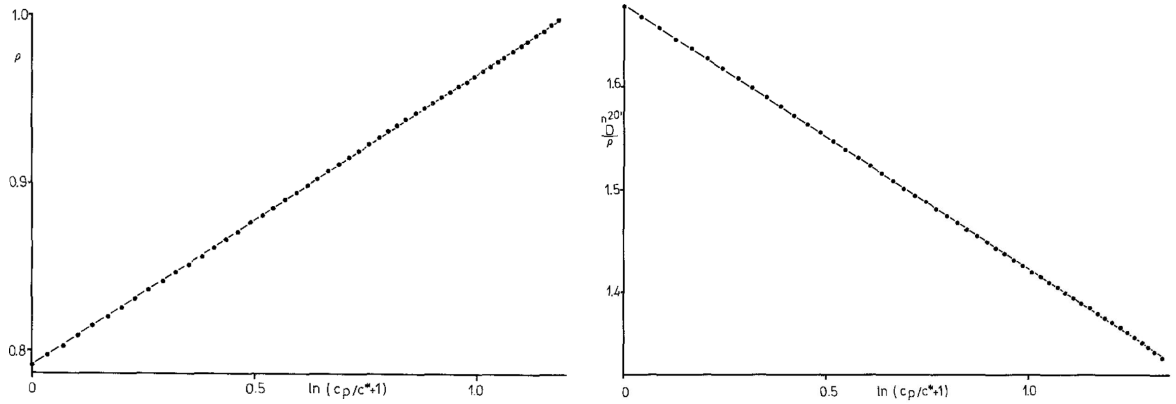

Figure 23. (**Left**) Linear correlation between the density ρ and ln (c_p/c^* + 1) according to Equation (5); every second measurement is recorded in the graphics for clarity (all measurements were used for calculations); slope 0.174, intercept 0.79093; c^* = 24.5, correlation number 0.999947 for 71 measurements; coefficient of determination 0.9999. (**Right**) Linear correlation between the index of refraction over the density ${n_D}^{20}/\rho$ and ln (c_p/c^* + 1) according to Equation (5); every second measurement is plotted for clarity; slope −0.257, intercept 1.6797; c^* = 19.9, correlation number −0.99998 for 71 measurements; coefficient of determination 0.99996.

16. Conclusions

The chemistry-dominating intermolecular interactions can be efficiently investigated by solvent polarity probes, whereby Dimroth and Reichardt's $E_T(30)$ scale certifies that because of the sensitivity of the optical method and other advantages, this essentially reflects the dipolarity of solvents; the polarizability of solvents is better characterized by Brooker's χ_R scale. Zelinski's universal polarity probe forms a link between both types of polarity scales because the fluorescence-dependent polarity scale S correlates linear with $E_T(30)$ for various solvents, while the absorbance of the dye correlates with Brooker's χ_R scale. Various solvent effects can be measured by means of multi-parameter approaches. Further insight into solvent effects and changes in the solvent structure were obtained by the developed two-parameter equation (5) for concentration-dependent effects. The equation includes condensed phases, binary mixtures where the property of one solvent can be continuously transformed into that of the other by changing the composition of the mixture, and even the effects in pure solvents with polar functional groups: The polar properties of media are dominated by polar groups or polar components, while other elements of structure or components essentially form the matrix. The appreciable thermochromism of **3** leading to a linear correlation between the $E_T(30)$ scale and the temperature (either in °C or K) was reported in relation to the thermal expansion of the solvent, with about 1/3 of the effect attributed to thermal expansion and 2/3 to temperature-induced breaking of hydrogen bonds; both effects are strongly linear with the temperature. Finally, very far-reaching intermolecular interactions were studied using the two-parameter equation (5) indicating intermolecular interactions of electronically excited states even for distances of more than 100 nm. Practical applications were shown for analytics both for the polarity probes and the two-parameter equation (5), the latter of which can be a useful tool for further investigations.

Funding: This research received no external funding.

Data Availability Statement: Not applicable.

Conflicts of Interest: The author declares no conflict of interest.

References

1. Smith, M.B.; March, J. *March's Advanced Organic Chemistry*, 6th ed.; John Wiley & Sons: Hoboken, NJ, USA, 2007; ISBN -13:978-0-471-72091-1.
2. Chandrasekhar, S. Stochastic Problems in Physics and Astronomy. *Rev. Mod. Phys.* **1943**, *15*, 1. [CrossRef]
3. Hunter, C.A. Quantifying Intermolecular Interactions: Guidelines for the Molecular Recognition Toolbox. *Angew. Chem. Int. Ed.* **2004**, *43*, 5310–5324. [CrossRef] [PubMed]
4. Langhals, H.; Schlücker, T. Dependence of the Fluorescent Lifetime τ on the Concentration at High Dilution. *J. Phys. Chem. Lett.* **2022**, *13*, 7568–7573. [CrossRef] [PubMed]
5. Langhals, H. Determination of the Concentration of Gases by Pressure Measurements. *Anal. Lett.* **1987**, *20*, 1595–1610. [CrossRef]
6. Michels, A.; Michels, C. Isotherms of CO_2 between 0° and 150° and pressures from 16 to 250 atm (Amagat densities 18-206). *Proc. Roy. Soc. London Ser. A* **1935**, *153*, 201–214. [CrossRef]
7. Michels, A.; Bijl, A.; Michels, C. Thermodynamic Properties of CO_2 up to 3000 Atmospheres between 25 and 150 °C. *Proc. Royal Soc. London Ser. A Math. Phys. Sci.* **1937**, *160*, 376–384.
8. Michels, A.; Michels, C. Series evaluation of the isotherm data of CO2 between 0 and 150 °C. and up to 3000 atm. *Proc. Royal Soc. London Ser. A Math. Phys. Eng. Sci.* **1937**, *160*, 348–357. [CrossRef]
9. Michels, A.; Michels, C.; Wouters, H. Isotherms of CO_2 between 70 and 3000 atmospheres (Amagat densities between 200 and 600). *Proc. Royal Soc. London. Ser. A Math. Phys. Eng. Sci.* **1935**, *153*, 214–224. [CrossRef]
10. Simon, A.; Peters, K. Single-crystal refinement of the structure of carbon dioxide. *Acta Cryst. B* **1980**, *B36*, 2750–2751. [CrossRef]
11. Michels, A.; Blaisse, B.; Michels, C. The isotherms of CO_2 in the neighbourhood of the critical point and round the coexistence line. *Proc. Royal Soc. London. Ser. A Math. Phys. Eng. Sci.* **1937**, *160*, 358–375. [CrossRef]
12. Grault, S.T.; Squires, R.R. Generation of Alkyl Carbanions in the Gas Phase. *J. Am. Chem. Soc.* **1990**, *112*, 2506–2516. [CrossRef]
13. Tian, Z.; Kass, S.R. Carbanions in the gas phase. *Chem. Rev.* **2013**, *113*, 6986–7010. [CrossRef] [PubMed]
14. Kharasch, M.S.; Reinmuth, O. *Grignard Reactions of Nonmetallic Substances*; Constable & Company Ltd.: London, UK, 1954; OCLC-No. 545586.
15. Berthelot, M.; Péan de Saint Gilles, L. *Recherches Sur Les Affinités. De la Formation Et de la Decomposition Des Éthers*; Mallet-Bachelier: Paris, France, 1862; pp. 385–422.
16. Menschutkin, N. Über die Geschwindigkeit der Esterbildung. *Z. Phys. Chem.* **1887**, *1*, 611–630. [CrossRef]
17. Menschutkin, N. Über die Affinitätskoeffizienten der Alkylhaloide. *Z. Phys. Chem.* **1890**, *5*, 589–600. [CrossRef]
18. Menschutkin, N. Beiträge zur Kenntnis der Affinitätskoeffizienten der Alkylhaloide und der organischen Amine. Zweiter Teil. *Z. Phys. Chem.* **1890**, *6*, 41–57. [CrossRef]
19. Menschutkin, N. Zur Frage über den Einfluss chemisch indifferenter Lösungsmittel auf die Reaktionsgeschwindigkeiten. *Z. Phys. Chem.* **1900**, *34*, 157–167. [CrossRef]
20. Feynman, R.P.; Leighton, R.B.; Sands, M. *The Feynman Lectures on Physics: Definitive Edition*; Addison-Wesley: New York, NY, USA, 2005; Volume 2, Chapter 11-5.
21. Kirkwood, J.G. The Dielectric Polarization of Polar Liquids. *J. Chem. Phys.* **1939**, *7*, 911–919. [CrossRef]
22. Langhals, H. Heterocyclic structures applied as efficient molecular probes for the investigation of chemically important interactions in the liquid phase. *Chem. Heterocycl. Compd.* **2017**, *53*, 2–10. [CrossRef]
23. Debye, P. Der Rotationszustand von Molekülen in Flüssigkeiten. *Physik. Zeits.* **1935**, *36*, 100–101.
24. Eucken, A.; Wicke, E. Grundriss der physikalischen Chemie. In *Akademische Verlagsgesellschaft*, 10th ed.; Geest & Portig: Leipzig, Germany, 1958.
25. Kragh, H. The Lorenz-Lorentz Formula: Origin and Early History. *Substantia* **2018**, *2*, 7–18. [CrossRef]
26. Birge, R.T. A New Table of Values of the General Physical Constants (as of August, 1941). *Rev. Mod. Phys.* **1941**, *13*, 233–239. [CrossRef]
27. Lorenz, L. Ueber die Refractionsconstante. *Ann. Der Phys.* **1880**, *247*, 70–103. [CrossRef]
28. Lorentz, H.A. *Collected Papers*; Martinus Nijhoff: The Hague, The Netherlands, 1936; Volume 2, pp. 1–119.
29. Nee, T.-W.; Zwanzig, R. Theory of Dielectric Relaxation in Polar Liquids. *J. Chem. Phys.* **1970**, *52*, 6353–6363. [CrossRef]
30. Heckmann, A.; Lambert, C.; Goebel, M.; Wortmann, R. Synthese und photophysikalische Eigenschaften einer neutralen organischen gemischtvalenten Verbindung. *Angew. Chem.* **2004**, *116*, 5976, *Angew. Chem. Int. Ed.***2004**, *43*, 5851. [CrossRef]
31. Amthor, S.; Lambert, C.; Dümmler, S.; Fischer, I.; Schelter, J. Excited Mixed-Valence States of Symmetrical Donor−Acceptor−Donor π Systems. *J. Phys. Chem. A* **2006**, *110*, 5204–5214. [CrossRef] [PubMed]
32. del Castillo, L.F.; Dávalos-Orozco, L.A.; García-Colín, L.S. Ultrafast dielectric relaxation response of polar liquids. *J. Chem. Phys.* **1997**, *106*, 2348–2354. [CrossRef]
33. Domínguez, M.; Caroli Rezende, M. Towards a unified view of the solvatochromism of phenolate betaine dyes. *J. Phys. Org. Chem.* **2010**, *23*, 156–170. [CrossRef]
34. Liptay, W.; Becker, J.; Wehning, D.; Lang, W.; Burkhard, O. The Determination of Molecular Quantities from Measurements on Macroscopic Systems.II. The Determination of Electric Dipole Moments. *Z. Naturforsch. A* **1982**, *37A*, 1396–1408. [CrossRef]
35. Winstein, S.; Grunwald, E.; Jones, H.W. The Correlation of Solvolysis Rates and the Classification of Solvolysis Reactions into Mechanistic Categories. *J. Am. Chem. Soc.* **1951**, *73*, 2700–2707. [CrossRef]

36. Fainberg, A.H.; Winstein, S. Correlation of Solvolysis Rates. III. *t*-Butyl Chloride in a Wide Range of Solvent Mixtures. *J. Am. Chem. Soc.* **1956**, *78*, 2770–2777. [CrossRef]
37. Winstein, S.; Fainberg, A.H. Correlation of Solvolysis Rates. IV.1 Solvent Effects on Enthalpy and Entropy of Activation for Solvolysis of t-Butyl Chloride. *J. Am. Chem. Soc.* **1957**, *79*, 5937–5950. [CrossRef]
38. Chapman, N.B.; Shorter, J. (Eds.) *Correlation Analysis in Chemistry—Recent Advances*; Plenum Press: New York, NY, USA; London, UK, 1978. [CrossRef]
39. Hammett, L.P. *Physical Organic Chemistry*, 2nd ed.; McGraw-Hill: New York, NY, USA, 1970; ISBN -10:0070259054.
40. Wilputte-Steinert, L.; Fierens, P.J.C. Etude cinétique des réactions de solvolyse IV. Discussion Générale. *Bull Soc. Chim. Belges* **1955**, *64*, 308–332. [CrossRef]
41. Kosower, E.M. The Effect of Solvent on Spectra. I. A New Empirical Measure of Solvent Polarity: Z-Values. *J. Am. Chem. Soc.* **1958**, *80*, 3253–3260. [CrossRef]
42. Dimroth, K.; Arnoldy, G.; von Eicken, S.; Schiffle, G. Beziehungen zwischen Farbe, Konstitution, Lösungsmittel und chemischer Reaktionsfähigkeit. Untersuchungen über N^+, N^--Betaine der Pyridinreihe. *Justus Liebigs Ann. Chem.* **1957**, *604*, 221–251. [CrossRef]
43. Dimroth, K. Über den Einfluß des Lösungsmittels auf die Farbe organischer Verbindungen. *Symp. Über Farbenchem. Angew. Chem.* **1960**, *72*, 782–784. [CrossRef]
44. John, W. Die Anwendung der Solvatochromie organischer Farbstoffe zur kolorimetrischen Analyse von Lösungsmittel- und insbesondere von Treibstoffgemischen. *Angew. Chem.* **1947**, *59*, 188–194. [CrossRef]
45. Schneider, W. Strukturchemische Zwischenstufen und ihre kontinuierliche Verschiebung durch Solvatbildung. *Angew. Chem.* **1926**, *39*, 412. [CrossRef]
46. Schneider, W.; Dobling, W.; Cordua, R. Über Mesomerie bei *N*-Oxyphenyl-pyridinium-Basen. *Ber. dtsch. Chem. Ges.* **1937**, *70B*, 1645–1665, *Chem. Abstr.***1937**, *31*, 53446. [CrossRef]
47. Dimroth, K.; Reichardt, C.; Siepmann, T.; Bohlmann, F. Über Pyridinium-N-Phenol-Betaine und ihre Verwendung zur Charakterisierung der Polarität von Lösungsmitteln. *Justus Liebigs Ann. Chem.* **1962**, *661*, 1–37. [CrossRef]
48. Available online: https://www.uni-marburg.de/de/fb15/arbeitsgruppen/ag-reichardt/et30-werte-prof-reichardt (accessed on 23 November 2023).
49. Taft, R.W.; Kamlet, M.J. The solvatochromic comparison method. 2. The. alpha.-scale of solvent hydrogen-bond donor (HBD) acidities. *J. Am. Chem. Soc.* **1976**, *98*, 2886–2894. [CrossRef]
50. Plenert, A.C.; Mendez-Vega, E.; Sander, W. Micro- vs Macrosolvation in Reichardt's Dyes. *J. Am. Chem. Soc.* **2021**, *143*, 13156–13166. [CrossRef] [PubMed]
51. Kessler, M.A.; Wolfbeis, O.S. ET(33), a solvatochromic polarity and micellar probe for neutral aqueous solutions. *Chem. Phys. Lipids* **1989**, *50*, 51–56. [CrossRef]
52. Langhals, H. The Polarity of Solutions of Electrolytes. *Tetrahedron* **1987**, *43*, 1771–1774. [CrossRef]
53. Reichardt, C.; Che, D.; Heckenkemper, G.; Schäfer, G. Syntheses and UV/Vis-Spectroscopic Properties of Hydrophilic 2-, 3-, and 4-Pyridyl-Substituted Solvatochromic and Halochromic Pyridinium *N*-Phenolate Betaine Dyes as New Empirical Solvent Polarity Indicators. *Eur. J. Org. Chem.* **2001**, *12*, 2343–2361. [CrossRef]
54. Langhals, H. Increasing the solubility of aromatic compounds. *Ger. Offen.* DE 3016764 (April 30, **1980**). *Chem. Abstr.* **1982**, *96*, P70417x.
55. Reichardt, C.; Harbusch-Görnert, E. Über Pyridinium-N-phenolat-Betaine und ihre Verwendung zur Charakterisierung der Polarität von Lösungsmitteln, X. Erweiterung, Korrektur und Neudefinition der ET-Lösungsmittelpolaritätsskala mit Hilfe eines lipophilen penta-*tert*-butyl-substituierten Pyridinium-*N*-phenolat-Betainfarbstoffes. *Liebigs Ann. Chem.* **1983**, *1983*, 721–743. [CrossRef]
56. Reichardt, C. Empirische Parameter der Lösungsmittelpolarität als lineare„Freie Entha1pie"-Beziehungen. *Angew. Chem.* **1979**, *91*, 119–131, *Angew. Chem. Int. Ed*. **1979**, *18*, 98–110. [CrossRef]
57. Reichardt, C. Solvatochromic Dyes as Solvent Polarity Indicators. *Chem. Rev.* **1994**, *94*, 2319–2358. [CrossRef]
58. Langhals, H.; Braun, P.; Dietl, C.; Mayer, P. How many molecular layers of polar solvent molecules control chemistry? The concept of compensating dipoles. *Chem. Eur. J.* **2013**, *19*, 13511–13521. [CrossRef]
59. Langhals, H. The rapid identification of organic colorants by UV/Vis-spectroscopy. *Anal. Bioanal. Chem.* **2002**, *374*, 573–578. [CrossRef]
60. Brooker, L.G.S.; Keyes, G.H.; Heseltine, D.W. Color and constitution. XI. Anhydronium bases of *p*-hydroxystyryl dyes as solvent polarity indicators. *J. Am. Chem. Soc.* **1951**, *73*, 5350. [CrossRef]
61. Brooker, L.G.S.; Craig, A.C.; Heseltine, D.W.; Jenkins, P.W.; Lincoln, L.L. Color and constitution. XIII. Merocyanines as solvent property indicators. *J. Am. Chem. Soc.* **1965**, *87*, 2443–2450. [CrossRef]
62. Bekárek, V.; Bekárek, V., Jr. Effect of medium on electronic spectra of 4-dimethylamino-ω-nitrostyrenes. Effective Kirkwood-Onsager functions of medium. *Coll. Czech. Chem. Commun.* **1987**, *52*, 287–298. [CrossRef]
63. Langhals, H. Untersuchung des Lösungsmitteleinflusses auf Absorption und Emission bei Fluoreszenzfarbstoffen. *Z. Phys. Chem.* **1981**, *127*, 45–53. [CrossRef]
64. Zmyreva, I.A.; Zelinsky, V.V.; Kolobkov, V.P.; Krasnickaja, N.D. Universal Scale fort the Action of Solvents Upon Electron Spectra of Organic Compounds. *Dokl. Akad. Nauk SSSR* **1959**, *129*, 1089–1092.

65. Kulinich, A.V.; Mikitenko, E.K.; Ishchenko, A.A. Scope of negative solvatochromism and solvatofluorochromism of merocyanines. *Phys. Chem. Chem. Phys.* **2016**, *18*, 3444–3453. [CrossRef] [PubMed]
66. Griffiths, T.R.; Pugh, D.C. Correlations Among Solvent Polarity Scales, Dielectric Constant and Dipole Moment, and Means to Reliable Predictions of Polarity Scale Values from Current Data. *Coord. Chem. Revs.* **1979**, *29*, 129–211. [CrossRef]
67. Mayer, U.; Gutmann, V.; Gerger, W. The acceptor number—A quantitative empirical parameter for the electrophilic properties of solvents. *Monatsh. Chem.* **1975**, *106*, 1235–1257. [CrossRef]
68. Gutmann, V. Solvent effects on the reactivities of organometallic compounds. *Coord. Chem. Rev.* **1976**, *18*, 225–255. [CrossRef]
69. Katritzky, A.R.; Fara, D.C.; Yang, H.; Tamm, K.; Tamm, T.; Karelson, M. Quantitative Measures of Solvent Polarity. *Chem. Rev.* **2004**, *104*, 175–198. [CrossRef]
70. Kamlet, M.J.; Abboud, J.L.; Taft, R.W. The solvatochromic comparison method. 6. The.pi.* scale of solvent polarities. *J. Am. Chem. Soc.* **1977**, *99*, 6027–6038. [CrossRef]
71. Catalán, J. Toward a Generalized Treatment of the Solvent Effect Based on Four Empirical Scales: Dipolarity (SdP, a New Scale), Polarizability (SP), Acidity (SA), and Basicity (SB) of the Medium. *J. Phys. Chem. B* **2009**, *113*, 5951–5960. [CrossRef] [PubMed]
72. Catalán, J.; Hopf, H. Empirical Treatment of the Inductive and Dispersive Components of Solute−Solvent Interactions: The Solvent Polarizability (SP) Scale. *Eur. J. Org. Chem.* **2004**, *2004*, 4694–4702. [CrossRef]
73. Koppel, A.; Palm, V.A. *Influence of the Solvent on Organic Reactivity*; Chapman, N.B., Shorter, J., Eds.; Advances in Linear Free Energy Relationships; Plenum Press: London, UK, 1972; pp. 203–280.
74. Weckwerth, J.D.; Vitha, M.F.; Carr, P.W. The development and determination of chemically distinct solute parameters for use in linear solvation energy relationships. *Fluid Phase Equilibria* **2001**, *183–184*, 143–157. [CrossRef]
75. Spange, S.; Weiß, N. Empirical Hydrogen Bonding Donor (HBD) Parameters of Organic Solvents Using Solvatochromic Probes—A Critical Evaluation. *ChemPhysChem* **2023**, *24*, e202200780. [CrossRef] [PubMed]
76. Cook, J.L.; Hunter, C.A.; Low, C.M.R.; Perez-Velasco, A.; Vinter, J.G. Solvent Effects on Hydrogen Bonding. *Angew. Chem. Int. Ed.* **2007**, *46*, 3706–3709. [CrossRef] [PubMed]
77. Cabot, R.; Hunter, C.A. Molecular probes of solvation phenomena. *Chem. Soc. Rev.* **2012**, *41*, 3485–3492. [CrossRef] [PubMed]
78. Acree, W.E., Jr.; Lang, A.S.I.D. Reichardt's Dye-Based Solvent Polarity and Abraham Solvent Parameters: Examining Correlations and Predictive Modeling. *Liquids* **2023**, *3*, 303–313. [CrossRef]
79. Schweig, A.; Reichardt, C. π-Elektronen-Dipolmoment eines Pyridinium-*N*-phenol-betains. *Z. Naturforsch.* **1966**, *21a*, 1373–1376. [CrossRef]
80. Liptay, W.; Schlosser, H.J.; Dumbacher, B.; Hünig, S. Die Beeinflussung der optischen Absorption von Molekülen durch ein elektrisches Feld. *Z. Naturforsch.* **1968**, *23a*, 1613–1625. [CrossRef]
81. Beard, M.C.; Turner, G.M.; Schmuttenmaer, C.A. Measurement of Electromagnetic Radiation Emitted during Rapid Intramolecular Electron Transfer. *J. Am. Chem. Soc.* **2000**, *122*, 11541–11542. [CrossRef]
82. Beard, M.C.; Turner, G.M.; Schmuttenmaer, C.A. Measuring Intramolecular Charge Transfer via Coherent Generation of THz Radiation. *J. Phys. Chem. A* **2002**, *106*, 878–883. [CrossRef]
83. Stiopkin, I.V.; Weeraman, C.; Pieniazek, P.A.; Shalhout, F.Y.; Skinner, J.L.; Benderskii, A. Hydrogen bonding at the water surface revealed by isotopic dilution spectroscopy. *Nature* **2011**, *474*, 192–195. [CrossRef] [PubMed]
84. Hodges, A.M.; Kilpatrick, N.W.; McTigue, P.; Pereram, J.M. The solvation potential at the interface between water and methanol + water mixtures. *J. Electroanal. Chem.* **1986**, *215*, 63–82. [CrossRef]
85. Bosch, E.; Rosés, M. Relationships between E_T Polarity and Composition in Binary Solvent Mixtures. *J. Chem. Soc. Faraday Trans.* **1992**, *88*, 3541–3546. [CrossRef]
86. Langhals, H. *Primary Methods of Generating Solar Power by Using the Targeted Modification of Fluorescent Systems. Translation of: Prinzipielle Wege für Die Gewinnung von Solarenergie Über Gezielte Modifizierung Fluoreszierender Systeme*; Habilitationsschrift; Albert-Ludwigs-Universität Freiburg: Freiburg, Germany, 1981. [CrossRef]
87. Langhals, H. Polarität binärer Flüssigkeitsgemische. *Angew. Chem.* **1982**, *94*, 739–749, *Angew. Chem. Int. Ed. Engl.***1982**, *21*, 724–733. [CrossRef]
88. Keutsch, F.N.; Saykally, R.J. Water clusters: Untangling the mysteries of the liquid, one molecule at a time. *Proc. Nat. Acad. Sci. USA* **2001**, *98*, 10533–10540. [CrossRef]
89. Langhals, H. Die quantitative Beschreibung der Lösungsmittelpolarität binärer Gemische unter Berücksichtigung verschiedener Polaritätsskalen. *Chem. Ber.* **1981**, *114*, 2907–2913. [CrossRef]
90. Makogon, Y.F. *: Hydrates of Hydrocarbons*; Penn Well Publishing Company: Tulsa, OK, USA, 1997; ISBN 0-87814-718-7.
91. Langhals, H. Ungewöhnliches Polaritätsverhalten binärer Flüssigkeitsgemische. *Nouv. Journ. Chim.* **1981**, *5*, 511–514.
92. Koppel, I.; Koppel, J. ET parameters of binary mixtures of alcohols with DMSO and acetonitrile. Synergetic solvent effect of high intensity. *Org. React.* **1983**, *20*, 523–546, *Chem. Abstr.***1984**, *101*, 110180.
93. Testoni, F.M.; Ribeiro, E.A.; Giusti, L.A.; Machado, V.G. Merocyanine solvatochromic dyes in the study of synergistic effects in mixtures of chloroform with hydrogen-bond accepting solvents. *Spectrochim. Acta Part A* **2009**, *71*, 1704–1711. [CrossRef] [PubMed]
94. Langhals, H. Polarität von Flüssigkeitsgemischen mit begrenzt mischbaren Komponenten. *Z. Phys. Chem.* **1987**, *268*, 91–96. [CrossRef]
95. Langhals, H. Polarity of Liquid Mixtures with Components of Limited Miscibility. *Tetrahedron Lett.* **1986**, *27*, 339–342. [CrossRef]

96. Langhals, H. Die Beschreibung der Polarität von Alkoholen als Funktion ihres molaren Gehalts an OH-Gruppen. *Nouv. Journ. Chim.* **1982**, *6*, 265–267, English translation: The description of the polarity of alcohols as a function of their molar content of OH groups.
97. Spange, S.; Weiß, N.; Mayerhöfer, T.G. The Global Polarity of Alcoholic Solvents and Water—Importance of the Collectively Acting Factors Density, Refractive Index and Hydrogen Bonding Forces. *Chem. Open* **2022**, *11*, e202200140. [CrossRef] [PubMed]
98. Tamura, K.; Yoshiaki Ogo, Y.; Imoto, T. Effect of pressure on the solvent polarity parameter: ET value. *Chem. Lett.* **1973**, *2*, 625–628. [CrossRef]
99. Dimroth, K.; Reichardt, C.; Schweig, A. Über die Thermochromie von Pyridinium-*N*-Phenol-Betainen. *Liebigs Ann. Chem.* **1963**, *669*, 95–105. [CrossRef]
100. Forsythe, W.E. *Smithsonian Physical Tables*, 9th ed.; Smithsonian Institution Press: Washington, DC, USA, 1969; ISBN-10 0874740150; ISBN 13 978-0874740158.
101. Förster, T. Energiewanderung und Fluoreszenz. *Naturwiss* **1946**, *33*, 166–175, *Chem. Abstr.***1947**, *41*, 36668. [CrossRef]
102. Valeur, B.; Berberan-Santos, M. Excitation Energy Transfer. In *Molecular Fluorescence: Principles and Applications*, 2nd ed.; Wiley-VCH: Weinheim, Germany, 2012. [CrossRef]
103. Langhals, H.; Schlücker, T. Reply to "Comment on 'Dependence of the Fluorescent Lifetime τ on the Concentration at High Dilution'": Extended Interpretation. *J. Phys. Chem. Lett.* **2023**, *14*, 1457–1459. [CrossRef]
104. Langhals, H.; Fritz, E.; Mergelsberg, I. Die Trocknung von *tert*-Butylhydroperoxid nach einem einfachen, erstmals gefahrlosen Verfahren. *Chem. Ber.* **1980**, *113*, 3662–3665. [CrossRef]
105. Langhals, H. The Quality Control of Alcoholic Components of Disinfectants by a Simple Colour Test. *S. Afr. J. Chem.* **2020**, *73*, 81–83. [CrossRef]
106. Langhals, H. Ein neues, unkompliziertes Verfahren zur Bestimmung der Zusammensetzung binärer Flüssigkeitsgemische. *Zeitschr. Analyt. Chem.* **1981**, *308*, 441–444. [CrossRef]
107. Langhals, H. Ein neues, unkompliziert auszuführendes Verfahren zur Bestimmung kleiner Konzentrationen an Wasser in organischen Lösungsmitteln. *Zeitschr. Analyt. Chem.* **1981**, *305*, 26–28. [CrossRef]
108. Langhals, H. Bestimmung der Zusammensetzung binärer Flüssigkeitsgemische mit Hilfe von Fluoreszenzmessungen. *Zeitschr. Analyt. Chem.* **1982**, *310*, 427–428. [CrossRef]
109. Langhals, H. Der Zusammenhang zwischen dem Brechungsindex und der Zusammensetzung binärer Flüssigkeitsgemische. *Z. Phys. Chem.* **1985**, *266*, 775–780, English translation: The relationship between the refractive index and the composition of binary liquid mixtures. [CrossRef]